



The mitochondrial mRNA-stabilizing protein SLIRP regulates skeletal muscle mitochondrial structure and respiration by exercise-recoverable mechanisms

Received: 6 February 2024

A list of authors and their affiliations appears at the end of the paper

Accepted: 4 November 2024

Published online: 13 November 2024

Check for updates

Decline in mitochondrial function is linked to decreased muscle mass and strength in conditions like sarcopenia and type 2 diabetes. Despite therapeutic opportunities, there is limited and equivocal data regarding molecular cues controlling muscle mitochondrial plasticity. Here we uncovered that the mitochondrial mRNA-stabilizing protein SLIRP, in complex with LRPPRC, is a PGC-1 α target that regulates mitochondrial structure, respiration, and mtDNA-encoded-mRNA pools in skeletal muscle. Exercise training effectively counteracts mitochondrial defects caused by genetically-induced LRPPRC/SLIRP loss, despite sustained low mtDNA-encoded-mRNA pools, by increasing mitoribosome translation capacity and mitochondrial quality control. In humans, exercise training robustly increases muscle SLIRP and LRPPRC protein across exercise modalities and sexes, yet less prominently in individuals with type 2 diabetes. SLIRP muscle loss reduces *Drosophila* lifespan. Our data points to a mechanism of post-transcriptional mitochondrial regulation in muscle via mitochondrial mRNA stabilization, offering insights into how exercise enhances mitoribosome capacity and mitochondrial quality control to alleviate defects.

Mitochondrial homeostasis and function are vital for skeletal muscle physiology, primarily influenced by the ability to meet energy demands through oxidative phosphorylation (OXPHOS) in mitochondria¹. A decline in mitochondrial function is associated with decreased muscle mass and strength in multiple conditions, including sarcopenia, type 2 diabetes (T2D), and cancer. Reduced muscle function adversely impacts health and quality of life^{1–9} and is associated with increased all-cause mortality. Mounting evidence suggests that improvements in mitochondrial metabolism contribute to the exercise-induced functional benefits, as mitochondrial preservation protects against the age-associated decline in skeletal muscle mass and performance^{10,11}. The beneficial effects of exercise training are more potent than any drug in preserving muscle mass and function, positioning exercise training as a frontline strategy for the prevention and

treatment of sarcopenia, T2D, and cancer^{12–14}. Viewing mitochondrial control through the lens of exercise biology is a strategy to gain new mechanistic insights into mitochondrial regulation, which is currently incompletely understood. With an aging population and no FDA/EMA-approved drugs to treat muscle functional decline, there is an urgent unmet need to identify potential treatment targets.

OXPHOS proteins are of dual origin and transcribed in spatially distinct cellular compartments. Nuclear (n)DNA encodes for the majority of OXPHOS proteins. Yet, 13 essential OXPHOS proteins are encoded by the small circular high-copy number mitochondrial DNA (mtDNA)^{15,16}. In non-muscle systems, a protein complex comprised of steroid receptor RNA activator stem-loop interacting RNA-binding protein (SLIRP) and the leucine-rich pentatricopeptide repeat containing protein (LRPPRC) mediates mitochondrial-mRNA (mt-mRNA)

stability and polyadenylation of most mtDNA-encoded OXPHOS transcripts^{17–21}. SLIRP and LRPPRC, encoded by nuclear DNA, are primarily targeted to mitochondria. In addition, SLIRP may also regulate nuclear receptors by binding to steroid receptor RNA activator²², and LRPPRC may activate nuclear genes through interaction with PGC-1α²³. Stabilization of mt-mRNA is critical for protein synthesis by the mitochondrial ribosome (mitoribosome). Yet, the mitoribosome comprises 82 mitoribosomal proteins encoded by nuclear genes, and 12S and 16S rRNAs, highlighting the requirement for intricate coordination between the processes of cytosolic and mitochondrial protein synthesis^{18,19}.

Despite the high mitochondrial abundance in skeletal muscle, the complex interaction between LRPPRC/SLIRP-mediated posttranscriptional processes, mitoribosomal translation, and mitochondrial function has not previously been studied in skeletal muscle. Elucidating the underlying mechanisms for stabilizing mt-mRNA could not only facilitate our understanding of the fundamental energy metabolism in muscle, but also aid intervention strategies for diseases associated with skeletal muscle mitochondrial defects.

Endurance exercise training potently increases mitochondrial mass in skeletal muscle, in part due to the increased synthesis of nDNA- and mtDNA-encoded mitochondrial proteins^{1,24}. Importantly, exercise training retains its ability to improve oxidative capacity not only in healthy individuals but also in patients with mtDNA mutations, with common PGC-1α-mediated mitochondrial adaptive responses shared between both groups¹³. These results suggest that exercise training induces adaptations to reinforce the mitochondria's ability to efficiently respond to increased energy demands, even in the presence of mtDNA mutations, which may negatively affect mitochondrial transcription and translation. However, a notable knowledge gap persists in understanding the role of mitochondrial posttranscriptional processes, specifically in mt-mRNA stabilization and translation, in skeletal muscle biology and following exercise training. Yet, that knowledge is needed to gain a comprehensive understanding of the adaptive responses to exercise training.

Since SLIRP, a key player in mitochondrial posttranscriptional gene expression, is markedly upregulated in mouse skeletal muscle by exercise training²⁵, we hypothesized that SLIRP would regulate mitochondrial function in skeletal muscle at rest and in response to exercise training. Our findings illuminate SLIRP's role in regulating mt-mRNA transcript levels in skeletal muscle, downstream of PGC-1αL. Knockout (KO) of SLIRP led to damaged and fragmented mitochondria alongside lowered respiration. Intriguingly, exercise training could compensate for the absence of SLIRP, leading to improvements in mitochondrial integrity and respiratory capacity. Our findings imply the activation of complex exercise-induced molecular signaling in skeletal muscle which bypasses mt-mRNA defects, possibly through enhanced mitoribosomal translation and capacity of mitochondrial quality control.

Results

SLIRP controls mt-mRNA levels and respiration in muscle

Protein profiling of five different skeletal muscle tissues showed that SLIRP content was highest in the oxidative soleus compared to glycolytic extensor digitorum longus (EDL, Fig. 1A, Supplementary Fig. 1A), in accordance with the potential critical role for SLIRP in oxidation. Moreover, SLIRP was present across a diverse array of tissues in mice and was highly abundant in energy-demanding tissues such as liver, kidney, brown adipose tissue, heart, and skeletal muscle (Fig. 1A, Supplementary Fig. 1A), in line with previously reported *Slirp* mRNA levels²².

In skeletal muscle of global *Slirp* KO mice, SLIRP protein was undetectable. Moreover, SLIRP's binding partner LRPPRC showed 90% reduction in protein content (Fig. 1B), indicative of their co-stabilization. To confirm co-stabilization, we administered

intramuscular injections of recombinant adeno-associated viral serotype 6 (rAAV6):*Slirp* into the *tibialis anterior* (TA) muscle of wild-type (WT) mice, while injecting a control vector into the contralateral TA muscle. As expected, in the absence of injecting vectors to concomitantly upregulate LRPPRC, total SLIRP protein content did not increase because endogenous SLIRP protein was degraded (Fig. 1C). These findings show that SLIRP and LRPPRC stabilize each other in skeletal muscle, aligning with findings from non-muscle tissue^{17,18,20}.

We next determined the role of SLIRP for mitochondrial structure in skeletal muscle, using the membrane potential probe, tetramethylrhodamine ethyl ester (TMRE +), in intact flexor digitorum brevis (FDB) muscle fibers of *Slirp* KO and littermate control wild-type (WT) mice. Interestingly, the finely interconnected mitochondrial network, obvious in WT fibers, was disrupted in *Slirp* KO muscle fibers, evident by a 30% increased mitochondrial fragmentation index (Fig. 1D). Transmission electron microscopy (TEM) analysis of gastrocnemius muscle provided further insights into the ultrastructural changes of mitochondrial morphology in *Slirp* KO (Fig. 1E). Half of the *Slirp* KO gastrocnemius muscles displayed reduced density of the matrix, disarray of the cristae, and substantial enlargement and vacuolation of intermyofibrillar (IMF) mitochondria (Fig. 1E). Quantitative analysis of the mitochondria showed that the percentage of damaged IMF mitochondria was increased (Fig. 1F). However, there were no significant alterations in the total number of IMF mitochondria (Fig. 1G). The percentage of damaged mitochondria in *Slirp* KO muscle varied between 2–20% of total mitochondria compared to <2% of damaged mitochondria in WT muscle (Fig. 1E, F). Other structural parameters of IMF mitochondria, such as mitochondrial area, aspect ratio, elongation, convexity, perimeter, sphericity, and diameter did not display any significant changes in *Slirp* KO muscles, likely due to heterogeneity in the extent of damage (Fig. 1F, Supplementary Fig. 1B–H).

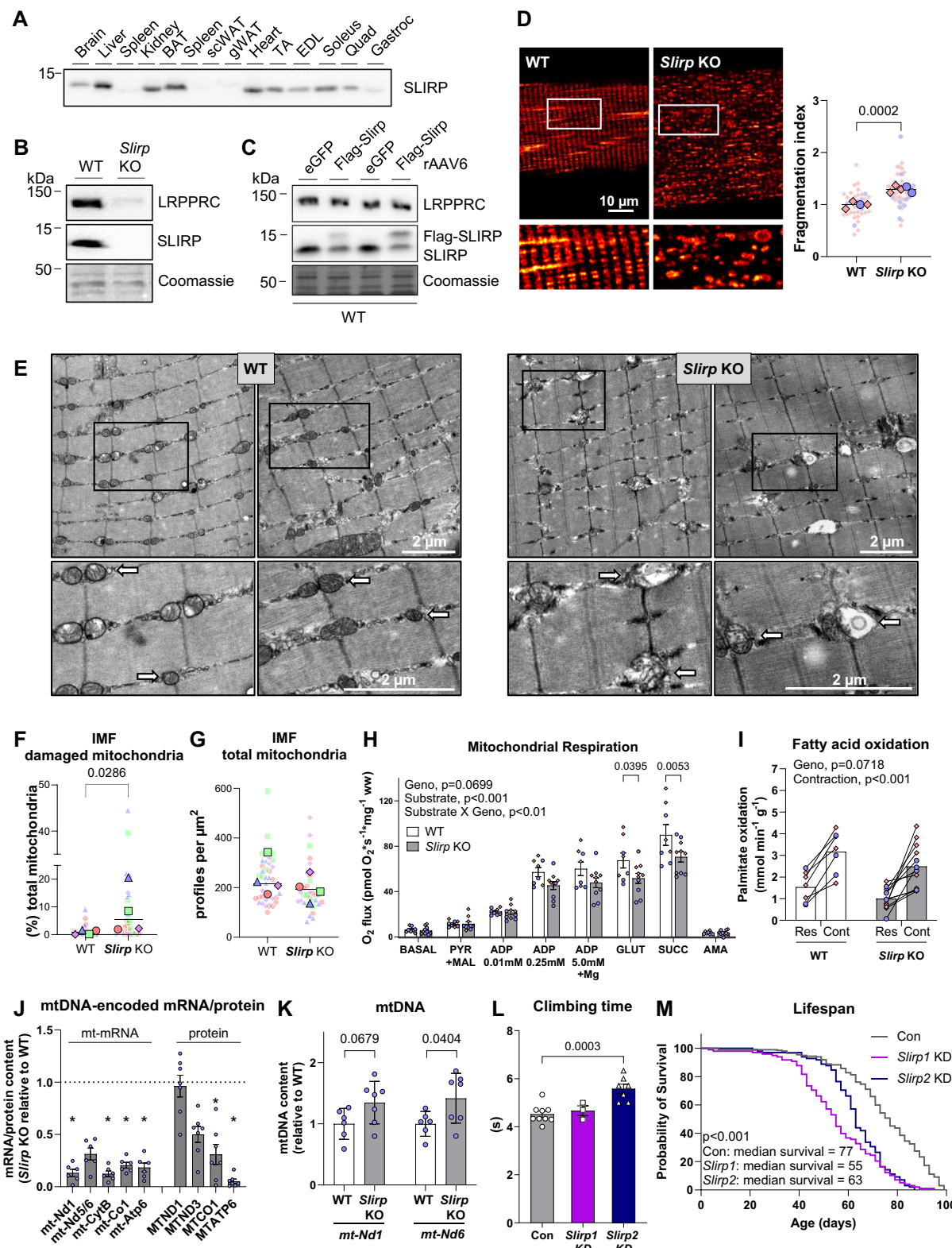
In agreement with the observable abnormalities in mitochondrial structure, respiratory capacity was reduced in permeabilized gastrocnemius muscle fibers of *Slirp* KO mice compared to WT (Fig. 1H). This was particularly evident when adding glutamate to assess complex I linked respiratory activity (~24%) and succinate to assess complex I + II linked respiratory capacity (~21%). These results indicate an important role for SLIRP selectively in skeletal muscle respiration, as in isolated mitochondria from liver and heart tissues, *Slirp* KO did not compromise mitochondrial respiration¹⁸. In agreement with lower respiration, fatty acid oxidation tended ($p = 0.0718$) to be lower in intact incubated soleus muscle of *Slirp* KO mice (Fig. 1I). However, electrically-induced muscle contraction increased fatty acid oxidation similarly in both genotypes, suggesting that fatty acid utilization for fuel during muscle contraction does not depend on SLIRP (Fig. 1I).

With the suggested role of SLIRP as an mt-mRNA stabilizing protein in non-muscle cells¹⁸, we determined mtDNA-encoded mRNA transcripts. Intriguingly, we observed a 60–80% reduction in *mt-Nd1*, *mt-Nd5/Nd6* (Complex I), *mt-CytB* (Complex III), *mt-Co1* (Complex IV), and *mt-Atp6* (ATP synthase) in gastrocnemius muscle (Fig. 1J) with concomitant reductions in protein content for MTCO1 and MTATP6. Additionally, there was an increased mtDNA copy number, estimated by measuring *Nd1* and *Nd6* (Fig. 1K). Those results indicate that SLIRP stabilizes mt-mRNA, and its loss adversely affects MTCO1 and MTATP6 protein content in skeletal muscle.

Together, these results suggest that mt-mRNA stabilization via SLIRP is required for proper mitochondrial network structure and morphology, and respiration in mouse muscle.

SLIRP regulates locomotion and lifespan in flies

To determine the long-term consequences of SLIRP muscle deficiency on the whole organism, we utilized the UAS-GAL4 system²⁶ for muscle-specific (*Mef2-GAL4* >) knock-down (KD) of *SLIRP1* and *SLIRP2* in *Drosophila* (*D. melanogaster*). Only one *SLIRP* gene is present in mouse and



human, while two *SLIRP* genes exist in *D. melanogaster* (Flybase annotation symbols (<http://flybase.org>): CG33714 and CG8021) likely to have originated from gene duplication events²⁷. This consequently gives rise to two fly orthologue proteins of the human and mouse *SLIRP*, denoted *SLIRP1* (CG33714) and *SLIRP2* (CG8021), respectively²⁷. The functions of the mammalian *SLIRP* are carried out by two proteins in flies: *SLIRP1* and *SLIRP2*, which interact with the fly orthologue proteins *LRPPRC1* and *LRPPRC2*, respectively, to regulate mt-mRNA

Polyadenylation and maturation, and coordinating mitoribosomal translation^{27–29}. To test physical functionality, we subjected the flies to a negative geotaxis (climbing) assay³⁰ and found that *SLIRP2* KD, but not *SLIRP1* KD, flies climbed 23% slower than control flies, indicative of impaired muscle function (Fig. 1L). The detrimental effects of *SLIRP* KD in the muscle became further apparent following starvation. Median fasting survival of *SLIRP1* KD flies was 41 h, compared with 44 h for control and *SLIRP2* KD flies (Supplementary Fig. 1I, $p = 0.0681$). Muscle-

Fig. 1 | *Slrp* knockout caused mild defects in mitochondrial structure and respiratory capacity, and reduced lifespan. **A** SLRP protein content across different wild-type tissues ($n = 3\text{--}4$, female C57BL/6J). **B** SLRP and LRPPRC protein content in tibialis anterior muscle of *Slrp* knockout (KO) and littermate wildtype (WT) mice; WT, $n = 26$; *Slrp* KO = 35. **C** SLRP and LRPPRC protein content in tibialis anterior muscle of WT mice injected with recombinant adeno-associated virus serotype 6 encoding SLRP (rAAV6:SLRP) or rAAV6:eGFP in the contralateral leg as control ($n = 6$). **D** Confocal microscopy of mitochondrial network structure in flexor digitorum brevis muscle fibers of *Slrp* KO and WT mice ($n = 4$, 7–10 fibers per mouse). Corresponding fragmentation index are presented as super plots¹⁰⁵; small symbols, each fiber; large symbols, mean of fibers per mouse and color- and symbol-coded for each sex (○ male, □ female). **E** TEM images of *Slrp* KO and WT gastrocnemius muscle ($n = 4$; 7–9 fibers per sample). **F, G** Quantification of percentage of damaged intramitochondrial (IMF) mitochondria within total mitochondria and relative volume of mitochondria. Small symbols, damaged or total mitochondria per fiber; large identical symbols, average of fibers per biological replicate (female *Slrp* KO and WT gastrocnemius muscle, $n = 4/\text{group}$). **H** Mitochondrial respiration in of *Slrp* KO and WT gastrocnemius muscle (male/

female: WT, $n = 4/4$; *Slrp* KO, $n = 5/5$); ○ (blue) male, □ (red) female. **I** Fatty acid oxidation in isolated *Slrp* KO and WT soleus muscle at rest and in response to contraction (male/female: WT, $n = 3/4$; *Slrp* KO, $n = 4/8$); ○ (blue) male, □ (red) female. **J** RT-qPCR analysis of mitochondrial transcript levels and corresponding immunoblots in gastrocnemius of male *Slrp* KO and WT mice (mRNA: WT, $n = 6$; *Slrp* KO, $n = 6$; protein: WT, $n = 6$; *Slrp* KO, $n = 7$). **K** qPCR analysis of mtDNA levels in male *Slrp* KO and WT mice (WT, $n = 6$; *Slrp* KO, $n = 7$). **L, M** Climbing assay and life span of control, *SLRP1* and *SLRP2* knockdown flies ($n = 3\text{--}9$, 10 flies per sample for climbing assay; $n = 10$, 10 flies per vial for lifespan assay). Data are shown as mean \pm SEM, including individual values, where applicable. Geno, main effect of genotype; substrate, main effect of substrate addition; Substrate X Geno, interaction between genotype and substrate; Contraction, main effect of contraction. * $p < 0.05$, ** $p < 0.01$, *** $p < 0.001$, as per Two-tailed Mann Whitney test (**D, F, G**) on average values, Two-way RM ANOVA with Šidák's multiple comparisons test (**H, I**), Two-tailed unpaired Student's *t* test (**J, K**), ordinary one-way ANOVA with Dunnell's multiple comparisons test (**L**), Log-rank (Mantel-Cox) test (**M**). Source data are provided as a Source Data file.

specific *SLRP* deficiency, irrespective of orthologue, had a deleterious effect on lifespan. While the median survival of control flies was 77 days, median survival of *SLRP1* and *SLRP2* KD flies was only 55 and 63 days, respectively, and accordingly both *SLRP1* and *SLRP2* KD significantly reduced lifespan (Fig. 1M).

Taken together these findings show that *SLRP* KD can have detrimental long-term consequences such as impaired muscle function, starvation intolerance, and reduced life span.

PGC-1 α 1 regulates training-induced muscle SLRP protein

Having established critical functional roles of SLRP in skeletal muscle mitochondrial morphology and respiratory capacity with detrimental effects on lifespan, we next investigated the upstream regulation of SLRP protein content. Our recent work pinpointed SLRP as a protein responsive to exercise training²⁵; yet the mechanisms governing its induction and functions remained elusive. Knowing that exercise potently increases PGC-1 α protein and mRNA levels in both mouse and human skeletal muscle^{31–34}, and that PGC-1 α is an important regulator of mitochondrial biogenesis, respiration, and quality control³⁵, we explored the regulation of SLRP by PGC-1 α . The *Ppargc1a* gene encodes several PGC-1 α isoforms, including isoform 1 (PGC-1 α 1) and isoform 4 (PGC-1 α 4), with distinct regulation and biological functions^{36,37}. Overexpression (OE) of PGC-1 α 1 in mouse skeletal muscle^{36,38}, associating with endurance exercise training-like adaptations^{36,38,39}, resulted in approximately 8.3-fold higher muscle SLRP protein content, without a concomitant change in *Slrp* mRNA levels (Fig. 2A). On the contrary, PGC-1 α 4 OE⁴⁰, inducing resistance-type exercise training adaptations such as muscle hypertrophy and strength³⁶, had no effect on SLRP protein content in mouse gastrocnemius muscle (Fig. 2B). This suggests that SLRP is an unrecognized player in PGC-1 α -regulated oxidative metabolism.

To test whether PGC-1 α regulates *Slrp* mRNA in skeletal muscle following exercise, we determined *Slrp* and *Ppargc1a* (Exon 3–5) mRNA levels in TA muscle 3 h into recovery from one exercise bout in mice lacking PGC-1 α in skeletal muscle (PGC-1 α mKO) and WT control littermates. *Slrp* mRNA was not upregulated 3 h post-exercise (Fig. 2C), in contrast to the expected³⁴ increase in *Ppargc1a* (+6.8-fold; Fig. 2C) in WT mice. Interestingly, *Slrp* mRNA levels were only modestly 14% reduced in PGC-1 α KO skeletal muscle (Fig. 2C), in line with the dissociation between *Slrp* mRNA levels and SLRP protein levels observed in PGC-1 α 1 OE skeletal muscle (Fig. 2A).

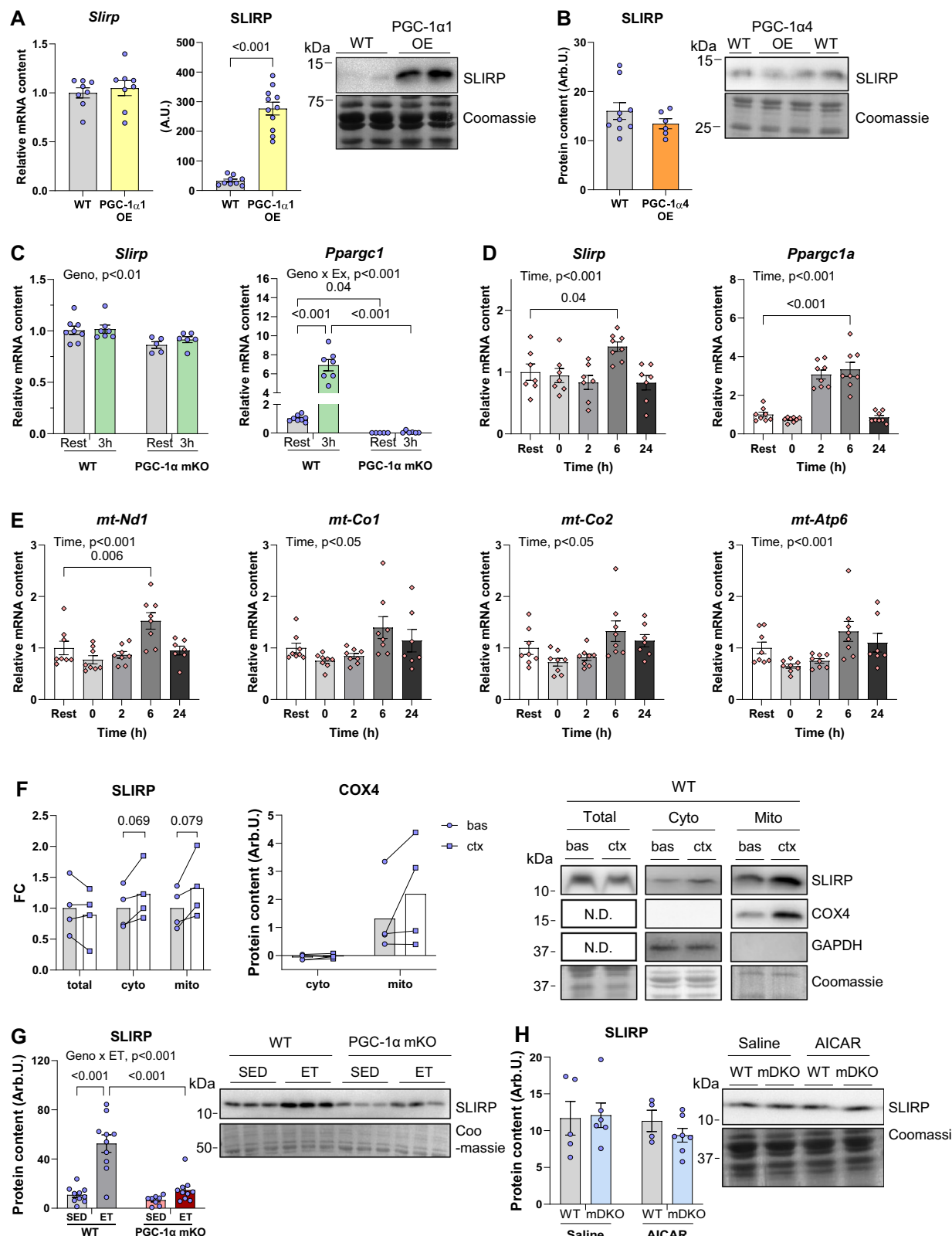
These findings align with reports describing only moderate correlations between mRNA and protein levels following exercise^{41–43}. Yet, with the interpretative limitations of a single post-exercise time point, we aimed to acquire a more detailed record of the temporal changes in *Slrp* transcripts in recovery from exercise. We subjected WT mice to

an acute exercise bout at 60% of their maximal running capacity and harvested quadriceps muscles at rest, immediately after, 2 h, 6 h, and 24 h post-exercise. We found that *Slrp* mRNA levels were 1.4-fold elevated 6 h into the recovery period in quadriceps muscle (Fig. 2D). This is a time-point not included in our prior cohort (Fig. 2C), and partially concurrent with *Ppargc1a* mRNA levels that were elevated 2 h (+3.0-fold) and 6 h post-exercise (+3.3-fold; Fig. 2D). Concomitant with *Slrp* and *Ppargc1a* mRNA levels, mtDNA-encoded *mt-Nd1* mRNA transcripts were increased 1.5-fold 6 h post-exercise, but not *mt-Cox1*, *mt-Cox2*, and *mt-Atp6* (Fig. 2E). These results indicate a coordinated regulatory mechanism linking SLRP, PGC-1 α and the simultaneous upregulation of *mt-Nd1* mRNA transcripts.

Since SLRP is a nuclear-encoded protein primarily targeted to mitochondria by a specific signal sequence, we next determined if muscle contractions increased the mitochondrial localization of SLRP in cytosolic and mitochondrial fractions. To investigate this, we investigated quadriceps muscles from WT mice 2 h after electrically-induced *in situ* contraction, using the contralateral leg muscle as a rested control, and performed an adapted subcellular fractionation assay on frozen tissue^{44,45} to isolate cytosolic and mitochondrial fractions. COX4 protein was used as mitochondrial marker, and GAPDH as cytosolic marker, respectively, to assess the purity of the fractions.

On a whole-tissue lysate level, SLRP protein remained unchanged in response to contraction (Fig. 2F). SLRP protein content tended to be 1.2-fold and 1.3-fold enriched in the cytosolic and mitochondrial fraction, respectively, following *in situ* muscle contraction (Fig. 2F), indicating that muscle contractions increase protein synthesis in the cytosolic and mitochondrial localization of SLRP. Interestingly, and with the same sample input, we were able to detect SLRP protein in the cytosolic fraction, indicating that SLRP may not be exclusive to mitochondria in skeletal muscle. These data suggest that muscle contraction elicits a subcellular redistribution of SLRP towards the mitochondria.

Given that SLRP might be regulated by PGC-1 α , we next turned to investigate the long-term dependency of exercise training-induced regulation of SLRP protein by PGC-1 α . In contrast to acute exercise, exercise training increased SLRP protein content 4.8-fold in WT mice (Fig. 2G), recapitulating our earlier observations in mice engaged in voluntary wheel running²⁵. The effect of exercise training on SLRP protein content was markedly blunted by 70% in mice lacking PGC-1 α in muscle compared to trained WT mice (Fig. 2G). Expectedly, in WT mice, exercise training potently upregulated the steady-state levels of multiple OXPHOS proteins including SDHB, UQCRC2, and MTCO1 in skeletal muscle (Supplementary Fig. 1I–K). In mice lacking PGC-1 α in muscle, SDHB (Supplementary Fig. 1I) and MTCO1 protein (Supplementary Fig. 1K) was 50–60% reduced in sedentary (SED) mice.



Moreover, the effect of exercise training on SDHB (Supplementary Fig. 1I) and UQCRC2 protein content (Supplementary Fig. 1J) was blunted by 30% and 65%, respectively, in PGC-1 α mKO compared to WT mice. In contrast to PGC-1 α , the exercise-sensitive metabolic sensor AMPK 46 did not seem to regulate SLIRP expression, as SLIRP protein abundance was comparable to controls in muscle-specific double KO

of AMPK α 1 and AMPK α 2 and WT mice 47,48 treated with or without the AMPK-activator AICAR for 4 weeks (Fig. 2H).

PGC-1 α has marked effects on muscle endurance, partially attributed to its pivotal role in mitochondrial biogenesis, and respiration 38,49 . Our results suggest SLIRP as an unrecognized downstream target of PGC-1 α in such exercise adaptations and oxidative metabolism.

Fig. 2 | SLIRP has increased mitochondrial localization upon exercise and is a target of PGC-1 α . A RT-qPCR analysis of *Slirp* transcript levels relative to *Actb* levels and Western blot analysis of SLIRP protein abundance in quadriceps with skeletal-muscle-specific transgenic expression of PGC-1 α (α1 OE; mRNA: $n = 8$ /group; protein: WT, $n = 9$; α1 OE, $n = 11$). B Western blot analysis of SLIRP protein abundance in gastrocnemius with skeletal-muscle-specific transgenic expression of PGC-1 α (α4 OE; WT, $n = 9$; α4 OE, $n = 6$). C RT-qPCR analysis of *Slirp* and *Ppargc1a* transcript levels relative to *Hprt* levels in gastrocnemius of muscle-specific PGC-1 α knockout (PGC-1 α mKO) and littermate control (WT) mice at rest and 3 h after acute exercise bout (WT, rest/3 h, $n = 8/7$; PGC-1 α mKO, rest/3 h, $n = 5/6$). D, E RT-qPCR analysis of *Slirp*, *Ppargc1a*, *mt-Nd1*, *mt-Co1*, *mt-Co2*, and *mt-Atp6*, transcript levels relative to *Actb* levels in WT quadriceps at rest, immediately after, 2 h, 6 h or 24 h after acute exercise bout ($n = 8$ /group). F Western blot analysis of SLIRP protein

content in whole-quadriceps lysate, and SLIRP and COX4 protein content in cytosolic and mitochondrial fractions, isolated from WT quadriceps at rest and 2 h after in situ contraction ($n = 4$ /group). G Western blot analysis of SLIRP protein abundance in quadriceps of sedentary (SED) and 12-week ET PGC-1 α mKO and WT mice (WT SED/ET, $n = 10/10$; PGC-1 α mKO SED/ET, $n = 8/10$). H Western blot analysis of SLIRP protein abundance in quadriceps of muscle-specific AMPK α 1 and - α 2 double KO (mDKO) and WT mice treated with/without AICAR (WT, saline/AICAR, $n = 5/4$; mDKO, saline/AICAR, $n = 6/7$). Data are means \pm SEM, including individual values. Geno, main effect of genotype; Ex, main effect of acute exercise; Geno x Ex, interaction between genotype and acute exercise. * $p < 0.05$, *** $p < 0.001$, as per Two-tailed unpaired Student's t test (A, B, F), Two-way ANOVA with Šídák's multiple comparisons test (C, G, H), and ordinary one-way ANOVA with Dunnett's multiple comparisons test (D, E). Source data are provided as a Source Data file.

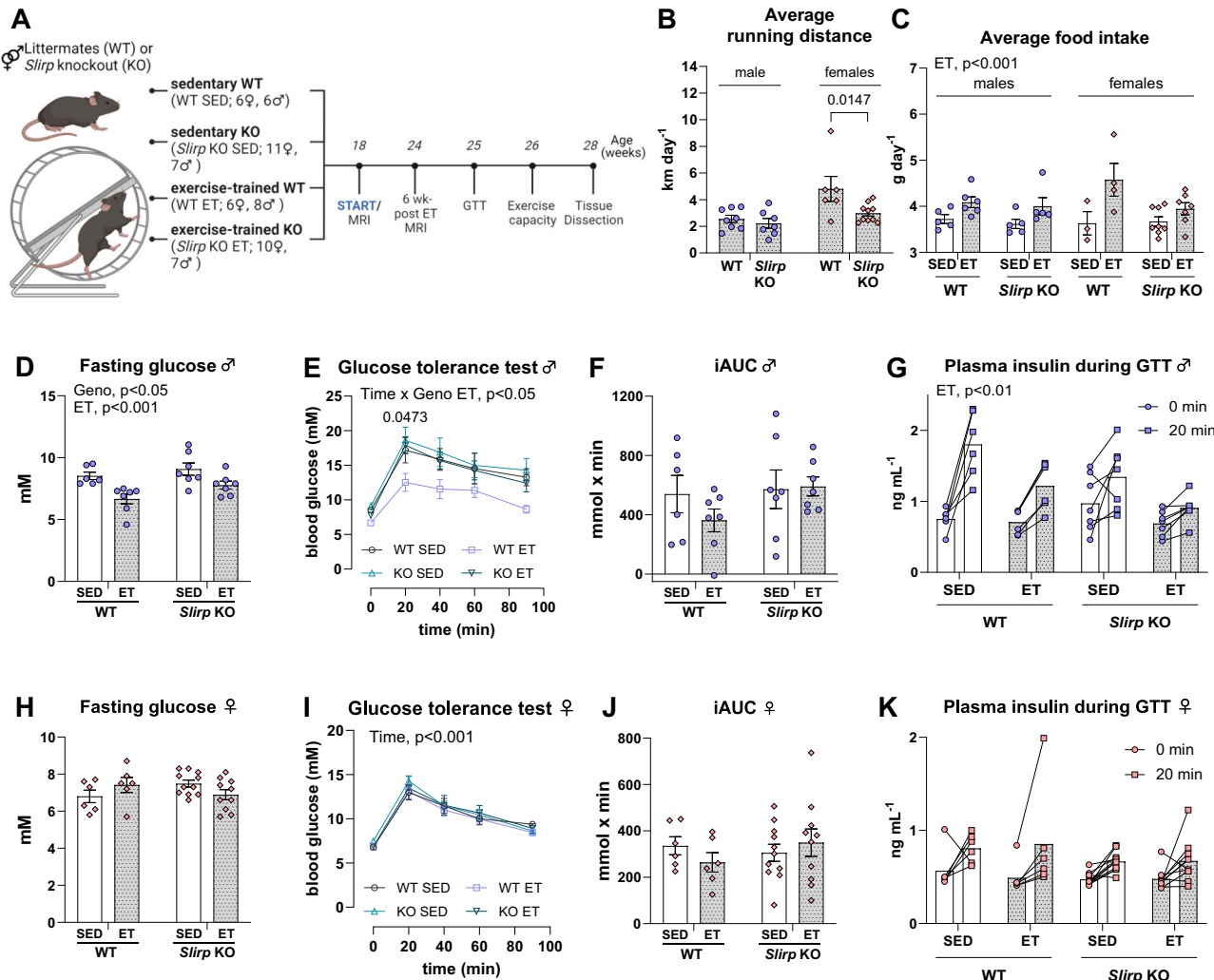


Fig. 3 | SLIRP is dispensable for organismal adaptations to ET, yet, needed for improving blood glucose regulation after ET in male mice. A Experimental design of 10-week exercise training (ET) intervention. Graphical illustration created in BioRender. Pham, T. (2023) BioRender.com/i39k213. B Average running distance of male and female ET *Slirp* KO or littermate control (WT) mice measured for 6 weeks (male/female: WT ET, $n = 8/6$; *Slirp* KO, $n = 7/10$; ○ (blue) male, ◇ (red) female). C Average food intake of male and female sedentary (SED) and ET *Slirp* KO or WT mice measured for 2 weeks after 4 weeks of running (male/female: WT SED, $n = 5/3$; WT ET, $n = 6/4$; *Slirp* KO SED, $n = 5/8$; *Slirp* KO ET, $n = 5/7$, ○ (blue) male, ◇ (red) female). D–K Blood glucose levels following a 4-hour fasting period before the glucose tolerance test (GTT). Glucose tolerance of male and female SED and ET

Slirp KO or WT mice after 7-weeks of ET. iAUC of glycemic excursion in response to bolus of glucose 2 g kg^{-1} body weight (BW). Insulin response before (0 min) and following (20 min) the oral glucose challenge (male/female: WT SED, $n = 6/6$; WT ET, $n = 7/6$; *Slirp* KO SED, $n = 7/11$; *Slirp* KO ET, $n = 7/10$. ○ male, ◇ female). Data are means \pm SEM, including individual values where applicable. Geno, main effect of genotype; ET, main effect of exercise training; Acute exercise, main effect of acute exercise bout; Time X Geno ET, interaction between glucose bolus and genotype in the ET groups. * $p < 0.05$, ** $p < 0.01$; E WT ET vs. KO ET, * $p < 0.05$; WT SED vs. WT ET, # $p < 0.05$, as per Two-tailed unpaired Student's t test (B), Two-way RM ANOVA with Šídák's multiple comparisons test in ET groups (E, I), Two-way ANOVA (C, D, F, G, H, J, K). Source data are provided as a Source Data file.

SLIRP dispensable for most adaptations to exercise training

Having identified SLIRP as an exercise training responsive protein downstream of PGC-1α, we next determined SLIRP's mechanistic involvement in exercise training-mediated organismal adaptations. To this end, we conducted a 10-week voluntary wheel-running training study in *Slirp* KO and WT littermate mice of both sexes commencing at ~18 weeks of age. The experimental design is shown in Fig. 3A.

The daily running distance recorded over 6 weeks of the 10-week study was 2.4 km/day on average for male mice of both genotypes, whereas it was 4.8 km/day for female exercise-trained (ET) WT mice and 3.0 km/day for female KO ET mice (Fig. 3B). It is important to consider that the running distance observed in our study of 18-week old mice is shorter than those reported in other exercise training studies using ~10-week-old mice, which typically run 6–8 km/day on average^{25,50,51}. Despite the higher food intake in ET mice (Fig. 3C), exercise training lowered body weight in both trained genotypes (Supplementary Fig. 2A). Moreover, irrespective of genotype, exercise training reduced fat mass/body weight ratio (Supplementary Fig. 2B) and increased lean mass/body weight ratio compared to sedentary (SED) groups (Supplementary Fig. 2C). Exercise training had no effect on gastrocnemius or TA muscle weight relative to tibia length in either sex (Supplementary Fig. 2D). However, we noted that female *Slirp* KO SED and both ET groups had elevated heart weight relative to WT SED (Supplementary Fig. 2D).

Exercise capacity increased similarly with exercise training, independently of genotype (+1.2-fold for WT ET, +1.3-fold for KO ET; Supplementary Fig. 2E) and sex (females shown in Supplementary Fig. 2G). Post-exercise blood lactate levels tended to be reduced (-1.7-fold; $p = 0.067$) by ET in WT male mice (Supplementary Fig. 2F). The training-induced lowering of blood lactate post-exercise was absent in male and female *Slirp* KO mice (Supplementary Fig. 2F, H).

Exercise training is a powerful preventative intervention against many metabolic disorders¹², partially due to its remarkable effects in improving glucose tolerance and insulin sensitivity documented in both animal models and humans^{25,50,52}. Accordingly, male WT ET mice displayed reduced fasting blood glucose (Fig. 3D) and improved blood glucose control evidenced by a downshifted glucose response curve compared to WT SED mice. This effect was not observed in trained male *Slirp* KO mice (Fig. 3E). Thus, trained *Slirp* KO mice displayed similar glucose tolerance as both SED groups. The incremental area under the curve (iAUC) of blood glucose was similar between groups (Fig. 3F), suggesting that the lowered plasma glucose excursion during the GTT was driven by lower basal glucose levels. Yet, exercise training reduced the levels of plasma insulin in both WT and *Slirp* KO mice, suggesting that insulin sensitivity was increased by exercise training in both groups (Fig. 3G). There was no effect of exercise training or genotype on fasting glucose, glucose tolerance or insulin levels in female mice (Fig. 3H–K).

Our results demonstrate that SLIRP is largely dispensable for organismal adaptations to exercise training, yet, in male mice SLIRP is required for training-induced improvement in blood glucose regulation.

Exercise training reverses *Slirp* KO mitochondrial defects

Exercise training can counteract mitochondrial damage, arising from excessive accumulation of reactive oxygen species (ROS) or impaired assembly of OXPHOS complex following mtDNA mutations^{11,13,53–55}. As we established that loss of SLIRP had marked negative implications for mitochondrial structure and respiration in skeletal muscle (Fig. 1E–H), we asked whether exercise training could rescue these defects.

Skeletal muscle mitochondrial network structure was qualitatively investigated in TMRE+ stained FDB fibers by confocal microscopy. Remarkably, exercise training completely rescued the derangements in mitochondrial network structure and mitochondrial fragmentation

observed in *Slirp* KO SED mice, quantitatively corroborated by restoration of the fragmentation index (Fig. 4A).

Concomitantly with improved mitochondrial structure, exercise training restored the respiratory flux in *Slirp* KO mice to the level of WT muscle (Fig. 4B). WT mice did not improve respiratory flux with exercise training, which was consistent with no effect of exercise training on fatty acid oxidation of contracting isolated WT soleus muscle (Supplementary Fig. 2I) and aligns with other studies^{56,57}. Exercise training in *Slirp* KO mice improved fatty acid oxidation in contracting *Slirp* KO soleus muscles (Supplementary Fig. 2I), in alignment with improved respiratory flux in *Slirp* KO muscles by exercise training. Thus, exercise training counteracted the structural alterations in *Slirp* KO SED mice and had a positive impact on mitochondrial respiratory capacity, suggesting restored mitochondrial function.

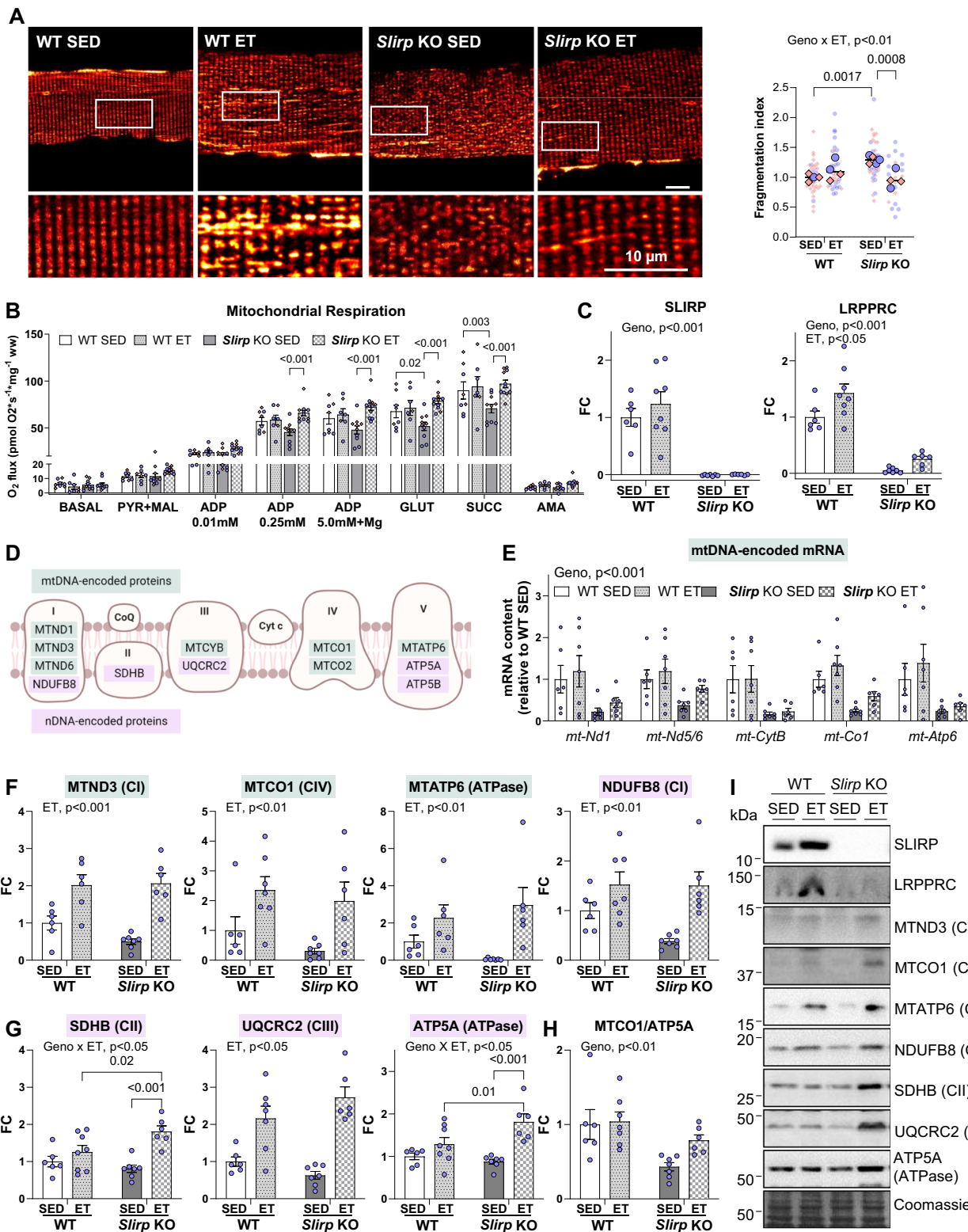
Together, these results support that exercise training exploits the remarkable adaptive plasticity that mitochondria retain even in the event of mitochondrial network disruptions and impaired respiratory flux in skeletal muscle.

Exercise training bypasses reduced mt transcript levels

We next aimed to investigate the molecular underpinnings for the defects in mitochondrial structure and function in *Slirp* KO and their correction by exercise training. We primarily focused our analyses on male mice, as our findings revealed a stronger propensity for adaptive response to exercise training in male *Slirp* KO mice. The corresponding analyses for female mice are included in Supplementary Fig. 3.

First, we verified that both SLIRP (+1.2-fold) and concomitantly LRPPRC (+1.4-fold) were upregulated by exercise training in the gastrocnemius muscle in WT, but not *Slirp* KO mice (Fig. 4C). These findings reinforce the co-stabilizing relationship of SLIRP and LRPPRC not only at sedentary^{17,18,20,58} but also during exercise trained conditions.

SLIRP, together with LRPPRC, has been shown to maintain mt-mRNA stability and aid mitoribosomal translation in non-muscle tissues^{17–20,58}. Indeed, the marked downregulation of mt-mRNA transcripts in SED *Slirp* KO muscle, also shown in Fig. 1J, remained largely reduced in ET *Slirp* KO mice relative to WT ET mice (Fig. 4E). Visually, there appeared to be a partial rescue of *mt-Nd5/6* and *mt-Co1* in ET *Slirp* KO mice, though this observation was not statistically confirmed. The sustained reduction in mt-mRNA transcripts upon *Slirp* KO is clearer in female mice, where exercise training significantly increased mt-mRNA transcript levels in WT mice, a response completely abrogated in *Slirp* KO mice (Supplementary Fig. 3B). The differences in mt-mRNA transcript levels in response to exercise training between sexes are likely due to the variation in running volume, with female WT mice running twice as much as male WT mice (4.8 km/day vs. 2.4 km/day; Fig. 3B). In contrast, mtDNA copy number, measured using quantitative PCR and primers for *mt-Nd1* (Supplementary Fig. 2J) or *mt-Nd5/mt-Nd6* (Supplementary Fig. 2K), were unaltered across groups or elevated only in *Slirp* KO SED mice. This suggests a compensatory response to mitigate muscle mitochondrial defects by increasing mtDNA copy number⁵⁹ or decreasing its degradation. Accordingly, these findings suggest that SLIRP is crucial for mitochondrial transcript stability in skeletal muscle. We were intrigued to find that exercise training still restored protein content of mtDNA-encoded OXPHOS subunits, MT-ND3, MT-CO1 and MT-ATP6 in *Slirp* KO mice (Fig. 4F). Thus, exercise training completely counteracted the sustained reduction in the mt-mRNA levels of these proteins in *Slirp* KO ET mice. Interestingly, exercise training markedly upregulated nuclear-encoded OXPHOS subunits SDHB (Complex II) and ATP5A (ATPase complex, also known as complex V) protein content in *Slirp* KO mice, both 1.4-fold more than in the trained WT mice (Fig. 4G). Other nuclear-encoded OXPHOS subunits, such as NDUFB8 (Complex I) and UQCRC2 (Complex III) also upregulated by exercise training (Fig. 4G, representative blots shown in Fig. 4I). Intriguingly, the trained *Slirp* KO mice had a more pronounced increase in all



OXPHOS protein content in response to exercise training compared to the WT mice (Supplementary Fig. 4A–G), suggesting a stronger propensity for adaptive responses to exercise training due to loss of SLIRP. Mitonuclear imbalance in *Slirp* KO mice also appeared to be restored by exercise training (Fig. 4H), evaluated by determining the ratio between mtDNA- (MTCO1) and nDNA-encoded (ATP5A) OXPHOS proteins⁶⁰. Citrate synthase (CS) activity correlates with mitochondrial content in human⁶¹ and mouse skeletal muscle⁶². CS activity, indicative of mitochondrial content, was increased similarly in *Slirp* KO and WT

mice after exercise training (Supplementary Fig. 2L), suggesting that improvements in mitochondrial content following exercise training are independent of SLIRP.

These results underline a substantial skeletal muscle mitochondrial plasticity, which is retained despite a 60–80% reduction in mt-mRNA pools. These findings point towards unidentified mechanisms by which exercise training modulates translational efficiency or protein degradation pathways to dictate final protein content.

Fig. 4 | Exercise training reverses SLIRP-induced defects in muscle mitochondrial structure and respiration despite sustained reductions of mitochondrial transcripts. **A** Confocal microscopy of mitochondrial network structure using a mitochondrial membrane potential probe (TMRE +) in flexor digitorum brevis muscle fibers of sedentary (SED) and 10-week ET *Slirp* knockout (KO) mice and littermate controls (WT) (male/female: WT SED, $n = 1/3$; WT ET, $n = 2/2$; *Slirp* KO SED, $n = 3/2$; *Slirp* KO ET, $n = 2/2$. 7–10 fibers per mouse, \circ male, \diamond female), and corresponding fragmentation index. SED data also depicted in Fig. 1D. **B** Mitochondrial respiration measured by Oroboros respirometry system in gastrocnemius of SED and ET *Slirp* KO and WT (male/female: WT SED, $n = 4/4$; WT ET, $n = 5/2$; *Slirp* KO SED, $n = 5/5$; *Slirp* KO ET, $n = 6/5$. \circ male, \diamond female). SED data is also depicted in Fig. 1H. **C** Western blot analysis of SLIRP and LRPPRC protein abundance in gastrocnemius of male SED and 10-week ET *Slirp* KO and WT mice (WT SED/ET, $n = 6/8$; *Slirp* KO SED/ET, $n = 7/6$). **D** Schematic of mtDNA- and nuclear

DNA-encoded oxidative phosphorylation (OXPHOS) proteins analysed. Graphical illustration created in BioRender. Pham, T. (2022) BioRender.com/n94e933. **E** RT-qPCR analysis of mitochondrial transcript levels in gastrocnemius of male SED and ET *Slirp* KO and WT mice (WT SED/ET, $n = 6/7$; *Slirp* KO SED/ET, $n = 7/6$). SED data also depicted in Fig. 1J. **F–H** Western blot analysis of (**F**) mtDNA-encoded proteins, MT-ND3 (CI), MT-CO1 (CIV), MT-ATP6 (ATPase), (**G**) nDNA-encoded proteins NDUFB8 (CI), SDHB (CII), UQCRC2 (CIII) and ATP5A (ATPase), (**H**) MTCO1/ATP5A ratio as readout of mitonuclear balance, and (**I**) representative blots in gastrocnemius of male SED and ET *Slirp* KO and WT mice (WT SED/ET, $n = 6/8$; *Slirp* KO SED, $n = 7/6$). Data are means \pm SEM, including individual values. Geno, main effect of genotype; ET, main effect of exercise training; Geno \times ET, interaction between genotype and exercise training; Substrate, main effect of substrate. * $p < 0.05$, ** $p < 0.01$, *** $p < 0.01$ as per Two-way ANOVA with Sídák's multiple comparisons test (**A, B, C, E, F–H**). Source data are provided as a Source Data file.

Exercise training increases mitoribosome mass and mt proteins

We next sought to determine the potential mechanism by which sustained reductions of mitochondrial transcript levels can be bypassed by exercise training. Enhanced mitochondrial protein synthesis mediates exercise training adaptations in muscle mitochondrial function in both young and elderly individuals⁴². Thus, we assessed pathways associated with protein synthesis in mitochondria, facilitated by the resident mitoribosomes. We observed training-induced increases in 12S ribosomal RNA (12S rRNA), 16S ribosomal rRNA (16S rRNA, Fig. 5B) and several mitoribosomal proteins, essential components of mitoribosome translation^{63,64} (MRPL11, MRPL12, MRPS18B, MRPS35, Fig. 5C). MRPL11, MRPL12, MRPS18B protein content was 86%, 59%, and 48%, respectively, more elevated in response to exercise training in *Slirp* KO than WT mice (Supplementary Fig. 4H–J). Exercise training increased cytosolic ribosomal protein S6 protein content 68% in WT mice and 34% in *Slirp* KO mice (rpS6, Fig. 5C; representative blots in Fig. 4L).

Given the predominant impact of *Slirp* KO on mitochondria, training-induced adaptive changes might also manifest directly within the affected cellular compartment. Here, we investigated mitochondrial quality control systems involving the mitochondrial Lon protease 1 (LONP1), YME1-like ATPase (YME1L1), the p-eIF2 α -ATF4-CHOP axis⁶⁵, and PRDX3.

LONP1 and YME1L1 are the frontline defense against mitochondrial damage and remove accumulated unfolded or damaged proteins⁶⁶. Exercise training increased both LONP1 and YME1L1 protein content (Fig. 5E, F), with a 1.7-fold greater response in *Slirp* KO mice (Supplementary Fig. 4K), suggesting an enhanced mitochondrial quality control induced by exercise training that is augmented in *Slirp* KO muscles with low mt-mRNA levels.

Recent research identifies mitochondrial damage as a key activator of the p-eIF2 α -ATF4-CHOP axis, known as integrated stress response (ISR)^{65,66}. Since ISR is involved in mitochondrial quality control, we measured EIF2 α phosphorylation at S51 to investigate the impact of SLIRP loss and exercise training on ISR. The loss of SLIRP tended to increase p-eIF2 α 1.4-fold, indicating the potential presence of mitochondrial damage. Intriguingly, exercise training markedly reduced phospho-eIF2 α by 58% selectively in *Slirp* KO mice, and below the level of WT SED and WT ET mice. As exercise training had no such effect in the WT mice (Fig. 5G, Supplementary Fig. 4L), exercise training may reduce phospho-eIF2 α specifically in the context of mitochondrial damage induced by SLIRP loss to promote protein translation.

Another mitochondrial quality control system involves a mitochondrial scavenger enzyme, peroxiredoxin 3 (PRDX3). PRDX3 plays a role in balancing redox environment specifically in mitochondria^{67,68}, possibly contributing to the preservation of factors critical for translation during conditions of mitochondrial dysfunction and exercise training. Interestingly, PRDX3 protein content was 50% lower in *Slirp* KO SED compared to WT SED mice, indicative of a lower mitochondrial

oxidative stress defense capacity in *Slirp* KO muscle. This was restored by exercise training, bringing PRDX3 up to levels observed in trained WT mice (Fig. 5I). We further noted that ET lowered the PRDX3 dimer to monomer ratio in both genotypes, indicative of a lower basal mitochondrial-derived peroxide accumulation likely due to an enhancement of scavenger activity (Fig. 5J). The cytosolic peroxiredoxin 2 (PRDX2) was unaffected by genotype and exercise training (Fig. 5K, representative blots in Fig. 5L).

Collectively, our findings indicate a complex interplay of spatially distinct molecular muscle adaptations in response to *Slirp* KO and ET. Our findings suggest that exercise training induces mechanisms to increase mitochondrial protein synthesis capacity and improve mitochondrial quality control. Specifically, exercise training elevated mitoribosome mass and restored mitochondrial quality control to powerfully circumvent the *Slirp* KO-induced depletion of mtDNA-encoded transcript levels.

Exercise elevates SLIRP and LRPPRC in human skeletal muscle

Our intriguing results from mouse and fly models prompted us to test whether our results provide translational value for humans in health and disease. SLIRP and LRPPRC protein content were determined in human skeletal muscle in four independent exercise cohorts employing different exercise modalities in conjunction with or without aging or diabetes and in males and females. Participant characteristics and study designs for the different ET modalities have been published previously for all the clinical studies^{69–72}.

Skeletal muscle SLIRP and LRPPRC protein abundances were 70% increased following 14-weeks of controlled and supervised aerobic and strength exercise training intervention in healthy young women⁶⁹ (Fig. 6A). Also, a 6-week high-intensity interval training (HIIT) intervention elevated muscle protein content of SLIRP (+80%, Fig. 6B) and LRPPRC (+50%, Fig. 6B) in healthy young men⁷². Thus, the exercise training response of SLIRP and LRPPRC was highly consistent, independent of sex, and responsive to various exercise modalities. The 12-week progressive resistance exercise training⁷⁰ increased SLIRP and LRPPRC muscle protein content in the entire group of young and old individuals but had no significant effect on LRPPRC abundance in neither young nor elderly subjects separately (Fig. 6C). The mtDNA-encoded transcript levels of MT-ND6, MT-CYB, MT-CO1 and MT-ATP6 were comparable across all groups (Fig. 6D), indicating that mitochondrial gene expression was not significantly affected by either aging or the training regimen in this study at the time of sampling. Similarly to our observations in mice, we observed a marked 1.9 and 2.3-fold increase in MRPL11 in elderly and young individuals, respectively (Fig. 6E; representative blot in Fig. 6C), supporting that the increase in mitoribosomal biogenesis and mitochondrial translation capacity in response to exercise training is conserved in humans⁴².

Exercise training-mediated improvements in muscle mitochondrial content and function may be associated with improved glucose

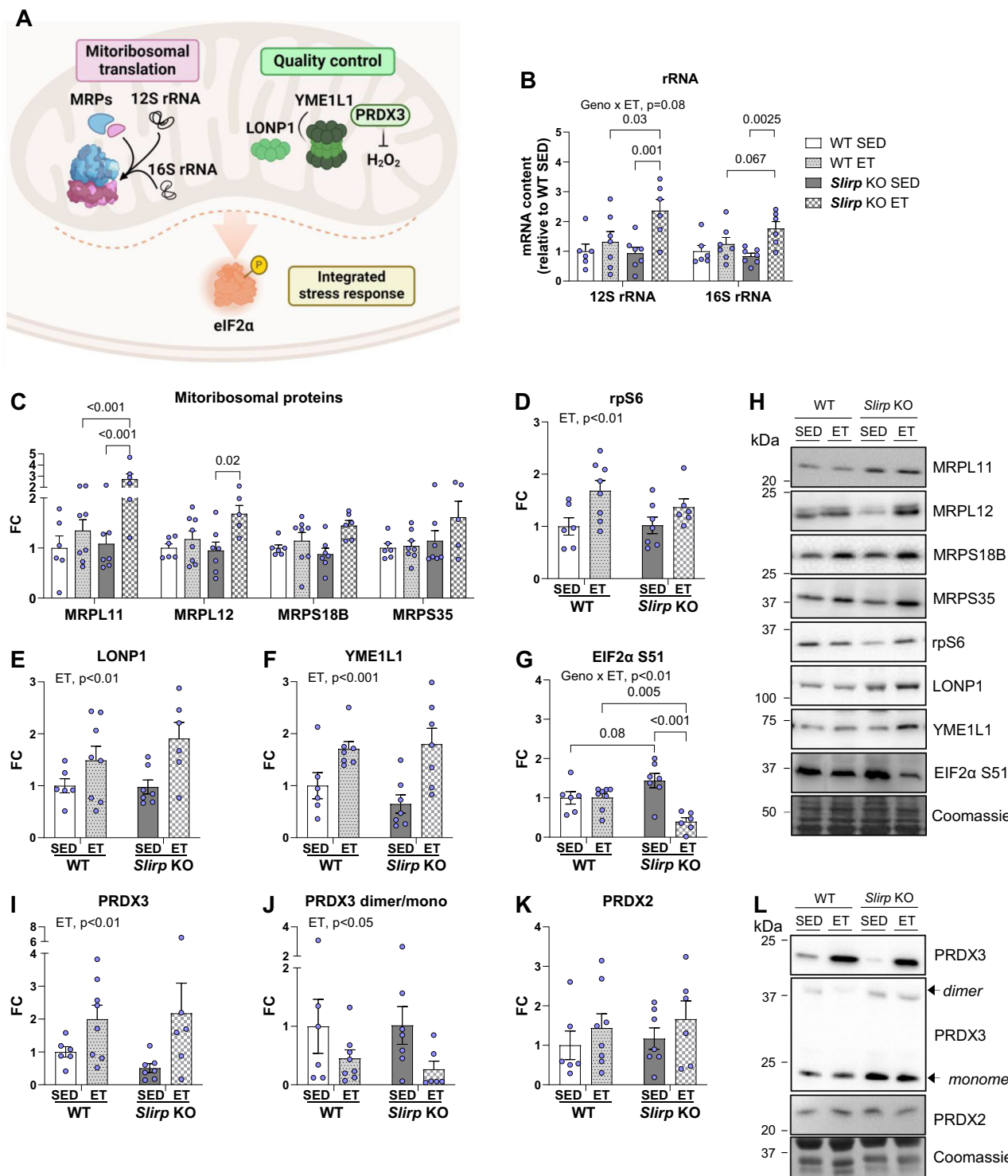
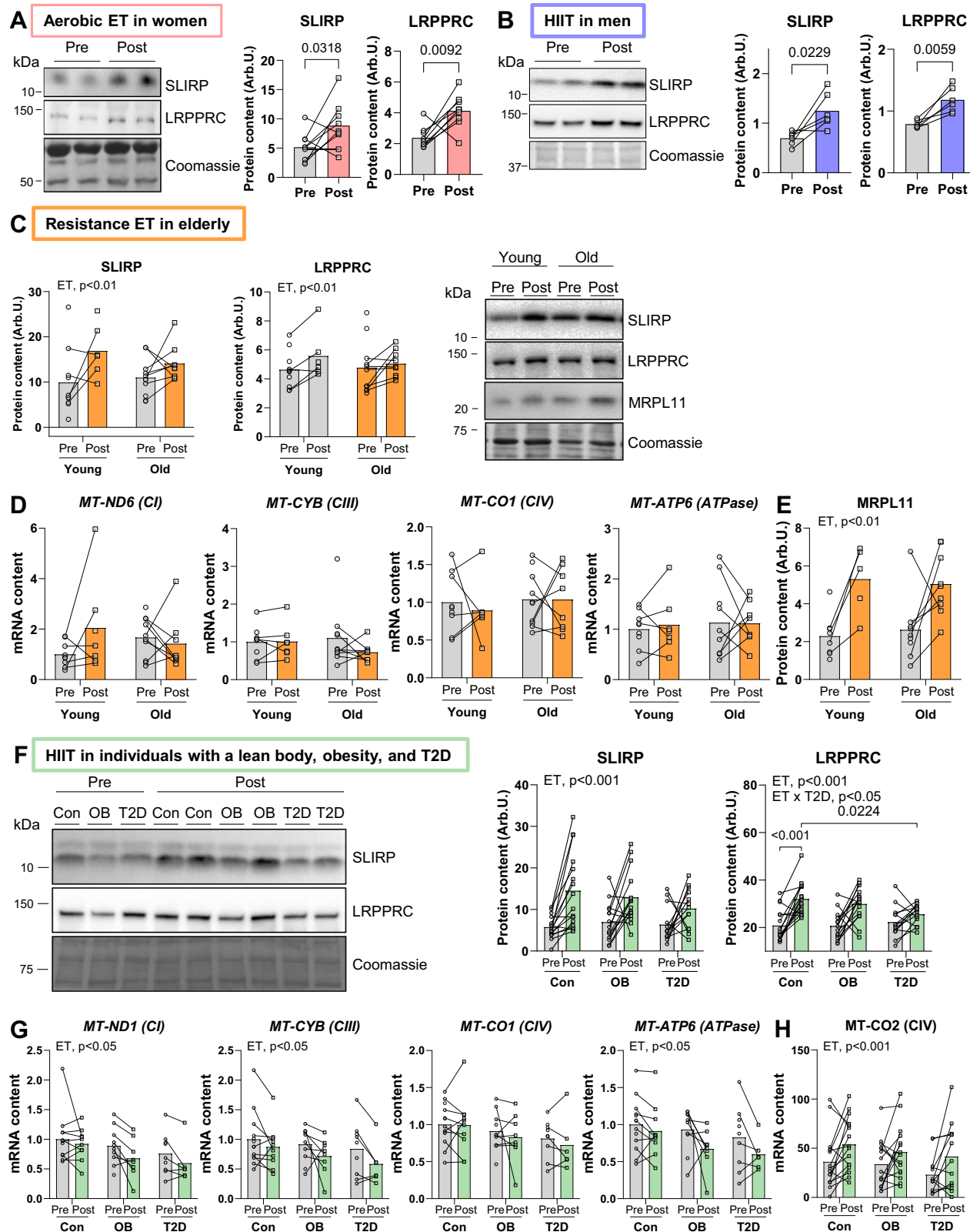


Fig. 5 | Exercise training increases mitoribosomal biogenesis and mitochondrial quality control. **A** Schematic of proteins associated with mitoribosomal biogenesis and mitochondrial quality control analysed. Graphical illustration created in BioRender. Pham, T. (2024) BioRender.com/y84d051. **B** RT-qPCR analysis of 12S rRNA and 16S rRNA in gastrocnemius of male sedentary (SED) and exercise trained (ET) *Slip* knockout (KO) and control littermate (WT) mice (WT SED/ET, n = 6/7; *Slip* KO SED/ET, n = 7/6). **C–L** Western blot analysis of mitoribosomal proteins (MRPL11, MRPL12, MRPS18B, MRPS35; C), rpS6 (D), LONP1 (E), YME1L1 (F), phospho-EIF2α S51 (G), PRDX3 (I), PRDX3 dimer/monomer ratio (J), PRDX2 (K), and representative blots (H, L) in gastrocnemius of male sedentary (SED) and exercise trained (ET) *Slip* knockout (KO) and control littermate (WT) mice (WT SED/ET, n = 6/8; *Slip* KO SED/ET, n = 7/6). Data are means ± SEM, including individual values. Geno, main effect of genotype; ET, main effect of exercise training; *p < 0.05, **p < 0.01, as per Two-way ANOVA (B–G, I–K). Source data are provided as a Source Data file.

metabolism in individuals with obesity and T2D^{73,74}, although this association is not always clear⁷⁵. The training response of muscle SLIRP and LRPPRC to 8-weeks HIIT was conserved in individuals who were lean (+150% and +54%) or obese (+85% and +45%, Fig. 6F). However,

the exercise response for LRPPRC, but not SLIRP, was blunted in muscle of patients with T2D in comparison to lean individuals (Fig. 6F), suggesting impaired sensitivity of muscle to some mitochondrial adaptations to ET in T2D. At the mRNA level, mt-DNA encoded



transcripts of *MT-ND1*, *MT-CYB*, *MT-CO1* and *MT-ATP6* were reduced with HIIT across all groups (Fig. 6G). Yet, protein content of *MT-CO2* (Fig. 6H, representative blot in Supplementary Fig. 5A) and other nuclear-encoded OXPHOS proteins (Supplementary Fig. 5A) were significantly upregulated with HIIT. In line with previous findings⁴², the upregulation in OXPHOS protein abundance occurred despite lower levels of mRNA, and demonstrate a disassociation between the

transcriptome and proteome⁷⁶. Our correlation analysis in this cohort revealed that SLIRP protein content was positively associated with LRPPRC ($r^2 = 0.2901$) and several OXPHOS proteins, specifically NDUFB8 ($r^2 = 0.1487$), SDHB ($r^2 = 0.4020$), UQCRC2 ($r^2 = 0.1110$), *MT-CO2* ($r^2 = 0.0528$), and ATP5A ($r^2 = 0.1141$, Supplementary Fig. 5).

Together, we show that SLIRP and LRPPRC are robustly upregulated in skeletal muscle across various exercise training modalities in

Fig. 6 | In human skeletal muscle SLIRP and LRPPRC protein content are increased by exercise training. A Western blot analysis of SLIRP and LRPPRC protein in the vastus lateralis muscle of healthy young women ($n = 9$ /group, (○ Pre ET, □ Post ET) before and after a 14-week controlled aerobic and strength exercise training (ET) intervention⁶⁹. B Immunoblotting of SLIRP and LRPPRC protein in the vastus lateralis muscle of healthy young men ($n = 6$ /group, (○ Pre ET, □ Post ET)) before and after a 6-week high intensity interval training (HIIT)⁷². C, E Immunoblotting of SLIRP and LRPPRC (C), MRPL11 (E) protein in the vastus lateralis muscle of male young and older individuals before and after 12-week progressive resistance training⁷⁰ (Young, Pre/Post, $n = 10/6$; Old, Pre/Post, $n = 11/9$. ○ Pre ET, □ Post ET). D RT-qPCR analysis of mitochondrial transcript levels in the vastus lateralis muscle of male young and older individuals before and after 12-week progressive resistance training⁷⁰ (Young, Pre/Post, $n = 9/7$; Old, Pre, $n = 10/8$. ○ Pre

ET, □ Post ET). F, H Immunoblotting of SLIRP, LRPPRC (F), and MT-CO2 (H) protein in the vastus lateralis muscle of glucose-tolerant lean, obese males, and males with type 2 diabetes before and after high-intensity interval training⁷¹ (Con, $n = 16$; OB, $n = 15$, T2D, $n = 13$; ○ pre ET, □ post ET). Con, control; OB, obese; T2D, Type 2 diabetes. G RT-qPCR analysis of mitochondrial transcript levels in the vastus lateralis muscle of glucose-tolerant lean, obese males, and males with type 2 diabetes before and after high-intensity interval training⁷¹ (Con, Pre/Post, $n = 13/10$; OB, Pre/Post, $n = 10/8$; T2D, Pre/Post, $n = 9/6$; ○ pre ET, □ post ET). Data presented as individual before-and-after values. ET, main effect of exercise training, ET x T2D, Interaction between exercise training and presence of type 2 diabetes in Con and T2D group; * $p < 0.05$, ** $p < 0.01$, *** $p < 0.001$, as per two-tailed paired Student's t test (A–C), Mixed-effects, REML model (D, E, G), Two-way RM ANOVA with Šidák's multiple comparisons test (F, H). Source data are provided as a Source Data file.

men and women, lean and obese. However, the exercise training response of LRPPRC was blunted in patients with T2D. This suggests that T2D is associated with decreased sensitivity to some of the adaptive mitochondrial responses normally elicited by exercise training, possibly influenced by exercise intensity or volume. Thus, our clinical data in humans provide strong translational value of the SLIRP-deficient fly and mouse models and point towards a conserved requirement of SLIRP for skeletal muscle health, and potentially the SLIRP-independent mechanisms that compensate during exercise training.

Discussion

Our investigation led to six key findings that bridge substantial knowledge gaps concerning the role of mitochondrial posttranscriptional mechanisms on skeletal muscle biology and their contributions to exercise training adaptations.

First, lack of *Slirp* led to mild mitochondrial network disruption, mitochondrial fragmentation, and reduced respiratory capacity in skeletal muscle in mice. Second, SLIRP deficiency impaired muscle functionality, and reduced lifespan in flies. Third, SLIRP was identified as an exercise training-responsive downstream target of PGC1- α . Fourth, SLIRP was needed for improving blood glucose regulation after exercise training in male mice. Fifth, exercise training restored the mitochondrial defects elicited by the lack of SLIRP on mitochondrial structure, respiration, and mtDNA-encoded OXPHOS, via mechanisms likely involving the upregulation of mitoribosome content and enhanced mitochondrial quality control. Finally, we established a translational foundation for our findings by substantiating the conservation of SLIRP's response to exercise training in four independent human cohorts integrating different exercise modalities, sex, health, and age conditions. These findings not only unravel a delicate interplay between the mt-mRNA-stabilizing protein SLIRP, and the integrity of skeletal muscle mitochondria structure and performance, but also underscore the potential of exercise training in promoting selective mitochondrial translation capacity and quality control to circumvent these mechanisms (graphical summary depicted in Fig. 7).

Our first finding indicates that SLIRP is a hitherto unrecognized player in regulating mitochondria content, structure, and respiration in skeletal muscle. Our results are partially consistent with reports in heart, liver, and kidney *Slirp* KO^{17,18,58} showing that SLIRP forms a complex with LRPPRC and is crucial for the maintenance of the mt-mRNA reservoir. Accordingly, our observation of mitochondria with abnormal cristae in *Slirp* KO muscle aligns with TEM micrographs of *Lrpprc* KO heart tissue¹⁹. However, despite the stark similarities, mitochondrial respiration was mildly compromised in *Slirp* KO skeletal muscle, but not in heart or liver¹⁸, underscoring SLIRP's functional importance within skeletal muscle relative to other tissues. In alignment, previous research further showed that *Slirp* KO skeletal muscle fibers have reduced sarcoplasmic reticulum Ca^{2+} storage capacity⁷⁷. Interestingly, the young full-body *Slirp* KO mice only have a mild

molecular phenotype and appear overall healthy, despite the significant decrease in mt-mRNA levels, respiration, and mitochondrial morphology. The effects of *Slirp* KO on mitochondrial morphology further seemed to be isolated to IMF mitochondria, whereas subsarcolemmal mitochondria were unaffected at this age. Yet, detrimental physiological long-term consequences are suggested by the flies lacking SLIRP given their much shorter life span. Thus, our present findings underscore the importance of SLIRP across various tissue types, with emphasis on its importance for normal skeletal muscle mitochondrial morphology and respiration, and overall mitochondrial health.

Our second finding that SLIRP depletion compromised climbing ability, impaired starvation tolerance, and reduced lifespan in flies, illustrates the detrimental functional consequences of lacking SLIRP long-term in the muscle tissue. SLIRP1 has been demonstrated to interact with the fly orthologue protein LRPPRC1 to regulate mitochondrial mRNA polyadenylation and maturation, while SLIRP2 interacts with LRPPRC2 to coordinate mitochondrial translation^{19,27,28}. It has been shown that SLIRP1/LRPPRC1 and SLIRP2/LRPPRC2 complexes in flies have distinct essential roles in the regulation of mtDNA expression. This distinction likely accounts for the varying impacts on climbing ability, starvation tolerance, and lifespan observed when SLIRP1 or SLIRP2 is lost. The effects of mitochondrial proteins on modulating life span are equivocal. Some report that the depletion of specific OXPHOS genes reduces life span, whereas others report no effect or an increase on life span in model organisms^{78–80}. The "Mitochondrial Threshold Effect Theory"⁸¹ posits that mild mitochondrial dysfunction allows normal physiology in model organisms until a threshold is reached. Beyond that, severe mitochondrial dysfunction can lead to premature aging, developmental arrest or even death^{82–84}. In support, introducing a heteroplasmic pathogenic mtDNA mutation in the tRNA^{Ala} gene into *Slirp* KO mice caused an aggravated mitochondrial translation defect, resulting in embryonic lethality and impaired growth of mouse embryonic fibroblasts⁸⁵. Our findings support an important role for SLIRP and mitochondrial function in maintaining normal lifespan because we observed reduced survival in muscle-specific SLIRP KD flies.

Our third finding was that PGC-1 α 1 modulated SLIRP protein, providing evidence for a new training-responsive PGC-1 α target in skeletal muscle. Interestingly, training-induced adaptations in mitochondrial proteins can occur independently of PGC-1 α 1 as the main regulator⁸⁶. In agreement with that, our fifth finding was that the training-induced improvements in mitochondrial function could bypass SLIRP deletion. These findings agree with other studies showing that exercise training can rescue mitochondrial dysfunction and elicit improvements in glucose homeostasis in mice and humans^{13,53,86,87}. Interestingly, SLIRP was required for the training-induced improvements in blood glucose regulation in trained male *Slirp* KO mice. The mechanism by which SLIRP influences glucose metabolism was not established in the present study, although this

could be due to decreased intramyocellular insulin signalling⁸⁸, reduced insulin-independent glucose uptake¹⁴, capillarization, and/or blood flow⁸⁹. Female mice did not improve their glucose tolerance in response to exercise training. Sexual dimorphism in response to metabolic challenges, including exercise training, has been frequently reported in mouse models^{90,91}. In both sexes, exercise training circumvented SLIRP to induce mitochondrial and metabolic adaptations in skeletal muscle, despite sustained low mitochondrial transcript levels. However, we observed differences in mechanisms by which male and female mice compensated for the lack of SLIRP, illuminating an exciting area for further investigation.

We were intrigued by the observation that exercise training could circumvent even 60–80% loss in mitochondrial-mRNA pools to upregulate mtDNA-encoded OXPHOS proteins. In other words, the beneficial effect of exercise training on mitochondrial oxidative phosphorylation and ATP provision is independent of a correction of mt-mRNA transcript levels and LRPPRC/SLIRP protein content. As mtDNA copy number was either increased in SED *Slirp* KO or unchanged in ET *Slirp* KO mice, these findings give rise to the possibility that mt-mRNAs are produced in excess *in vivo*¹⁸. Excess mt-mRNA may allow for rapid engagement of mitochondrial protein synthesis in the event of sudden changes in energy demand. In response to exercise training, the mitoribosomal components, MRPL11, MRPL12, MRPS18B, *12S rRNA*, and *16S rRNA* were upregulated, indicating increased mitoribosome biogenesis and capacity for mitochondrial protein synthesis. These adaptations to exercise training may help sustain protein synthesis and normal physiology, even in the presence of low mt-mRNA abundance. The greater increase in OXPHOS, mt-mRNA, and mitoribosomal proteins in *Slirp* KO ET mice indicates that exercise training may be more effective in the presence of mitochondrial dysfunction, providing exciting avenues for exploring the use of exercise training in conditions of mitochondrial dysfunction. Exercise training also upregulated LONP1 and YME1L1, both important regulators of mitochondrial quality control and proteostasis, and PRDX3, linked to peroxide scavenging. While mitoribosomal protein content, *12S rRNA*, *16S rRNA*, LONP1, YME1L1, and PRDX3 may not directly control translation efficiency, their roles in the mitoribosomal makeup and improved mitochondrial quality control can influence the overall cellular environment where protein synthesis occurs. Albeit limited by not directly measuring mitochondrial translational rate, this working hypothesis is supported by findings in human skeletal muscle showing that mitochondrial protein synthesis and upregulation of mitoribosome biogenesis is at the core of exercise training-induced benefits⁴². That mitochondrial stress was effectively relieved via exercise training is suggested by the marked reduction in phosphorylation of EIF2a at S51, an integral marker of the ISR selectively in *Slirp* KO mice. This suggests a unique interaction between mitochondrial damage and the ISR, highlighting the heightened sensitivity of *Slirp* KO mice to exercise training.

Finally, our results are prospectively relevant to humans, as SLIRP and LRPPRC were consistently upregulated in human skeletal muscle in response to multiple exercise training modalities in both sexes. The effect of HIIT was blunted for LRPPRC in patients with T2D. Interestingly, the age-related decline in muscle mitochondrial protein synthesis⁹² can be reversed by exercise training in elderly⁴², corroborating our findings that ET bypasses SLIRP to increase mitoribosomal translation. Importantly, our findings demonstrate that the synthesis of mtDNA-encoded OXPHOS proteins is not limited by transcript abundance in skeletal muscle – a feature that seems to be conserved as a fundamental mechanism^{27,42}.

Taken together, our findings not only imply that mt-mRNA stabilization via SLIRP/LRPPRC is needed for the regulation of basal mitochondrial function in skeletal muscle, but also highlight an incredible exercise training-stimulated plasticity of mitochondria in skeletal muscle facing mitochondrial defects (graphical summary

depicted in Fig. 7). Our findings underscore exercise training as a therapeutic intervention to combat mitochondrial dysfunction in genetic and lifestyle-induced muscle pathologies, including T2D.

In this work, we uncover a conserved role for mitochondrial transcript stability via SLIRP in mitochondrial structure and respiratory capacity in skeletal muscle. We identify SLIRP as an exercise-responsive downstream target of PGC-1α that is conserved in human skeletal muscle and critical for lifespan in *Drosophila*. Because the defects in *Slirp* KO muscle could be reversed by ET, these findings add to the clinical relevance and add impetus to the important health-promoting role of ET in pathologies characterized by mitochondrial defects.

Methods

All research complies with all relevant ethical regulations

Clinical experiments were approved by the Ethics Committee of Copenhagen (H-17004045, H-2-2010-100, H-1-2013-034) or by the Regional Scientific Ethical Committees for Southern Denmark (S-20170142) and performed in accordance with the Helsinki Declaration II and with informed consent was obtained from all human research participants. No compensation was given to the study participants, apart from NCT02429128 and NCT03317704 where subjects received a small compensation for discomforts related to the study and were reimbursed for travel expenses. Studies including human study participants are described in refs. 69–72 and registered at ClinicalTrials.gov (NCT03500016, NCT02429128, NCT01252381, and NCT03317704). All mouse experiments complied with the European Convention for the protection of vertebrate animals used for experimental and other scientific purposes (No. 123, Strasbourg, France, 1985; EU Directive 2010/63/EU for animal experiments) and were approved by the Danish Animal Experimental Inspectorate (License number: 2016-15-0201-01043, 2021-15-0201-01104).

Fly maintenance

In standard conditions, the flies were maintained on a SYA medium containing 0.5% (w/v) agar, 2.4% (v/v) nipagin, 0.7% (v/v) propionic acid, 10% (w/v) dry baker's yeast and 5% (w/v) sucrose. The experiments took place at +25 °C, 65% humidity under a 12 h:12 h light:dark cycle. RNAi lines for *SLIRP1* (51019 GD), *SLIRP2* (23675 GD), and the GD library control line (w1118, 60000 GD) were obtained from Vienna *Drosophila* Resource Center. Mef2-GAL4 line was obtained from Bloomington Stock Center to generate muscle-specific *SLIRP* KD flies.

Negative geotaxis (climbing) assay

Drosophila has a natural tendency to climb upwards, also known as negative geotaxis. The negative geotaxis, or climbing, assay was performed as previously described⁹³. Briefly, 20 male *Drosophila* flies aged 5–6 days were transferred into empty vials (25 × 95 mm), and another empty vial was taped on top to create a 25 × 190 mm cylinder. Six cylinders were set side by side into an apparatus. The apparatus was tapped down 5 times to make all the flies fall to the bottom of the cylinder. The climbing assay was measured in technical triplicate for each biological replicate, with 90 s allowed for each climb. The assay was recorded with a camera and videos were analysed to determine the time for half of the flies in the vial to reach halfway point (95 mm) in the cylinder.

Starvation assay using the *Drosophila* Activity Monitoring System (DAMS)

Four-day old male flies were individually housed in monitor tubes with an outside diameter of 5 mm (PPT5x65, Trikinetics, Waltham, MA). For starvation analysis, the tubes contained 1% agar in water. Thirtytwo tubes per monitor (DAM2 *Drosophila* Activity Monitor, Trikinetics, Waltham, MA) were set up, one monitor per genotype. For the starvation analysis, flies were kept in the DAM system until the last fly had died.

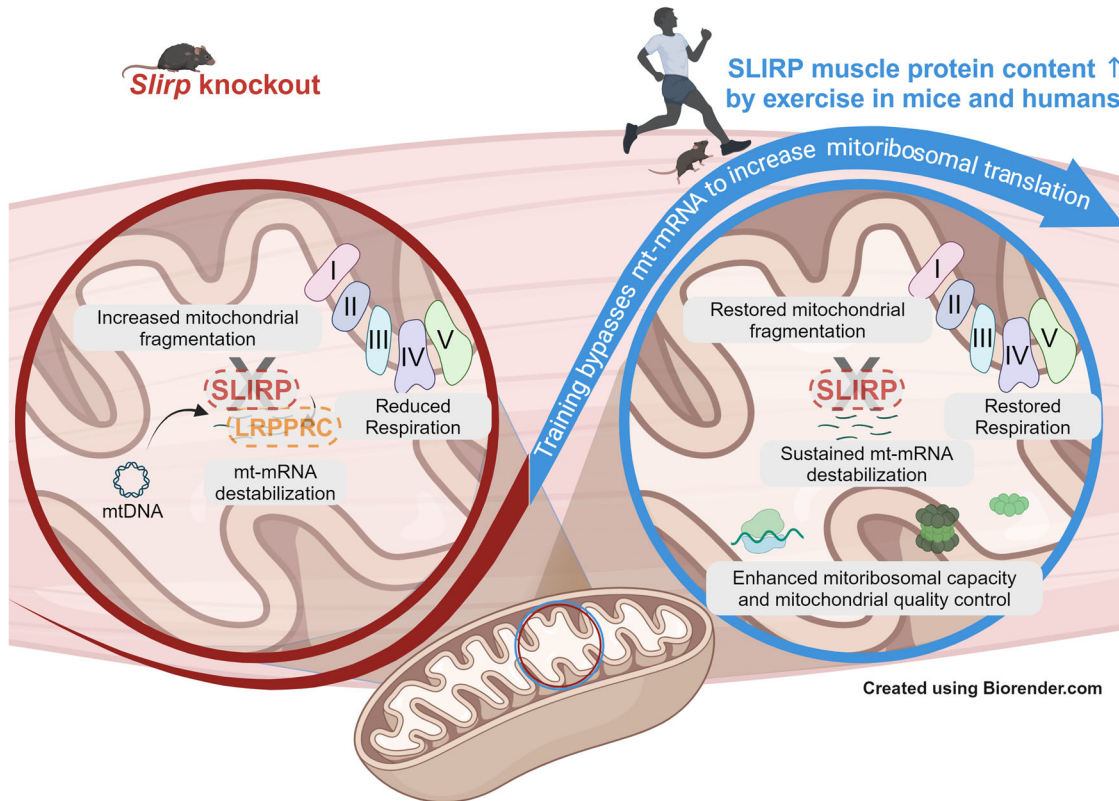


Fig. 7 | Illustration of findings obtained in the current study. Graphical illustration created in BioRender. Pham, T. (2023) BioRender.com/m15m010.

Lifespan assay

For lifespan assays, flies were mated at a controlled density of 25 female and 10 male flies, respectively. One-day old male flies were collected into vials (10 male flies per vial, with 10 vials per genotype). The flies were kept on a SYA diet in Drosoflippers (<http://www.drosofliper.com/>). Flies were flipped onto fresh food every second day and deaths were scored during the transfer.

Mice

PGC-1 α 1 transgenic mouse (PGC-1 α 1 OE). The generation of the model, quality, and specificity of the overexpression has been described previously³⁸, of which we analyzed quadriceps muscle samples of 12-week-old male WT and PGC-1 α 1 transgenic mice, kept on C57/Bl6 background.

PGC-1 α 4 transgenic mouse (PGC-1 α 4 OE). The generation of the model, quality, and specificity of the overexpression has been described previously³⁶, of which we analyzed gastrocnemius muscle samples of 12-week-old male WT and PGC-1 α 4 transgenic mice, kept on C57/Bl6 background.

Skeletal muscle-specific PGC-1 α knockout (PGC-1 α mKO). The generation of the model, quality, and specificity of the KO has been described previously⁴⁹. Male muscle-specific PGC-1 α MKO mice and littermate control mice homozygous for loxP inserts (lox/lox) were generated by crossbreeding myogenin-Cre mice with loxP flanked-Pgc-1 α mice. Mice were housed in a 12:12 h light/dark photocycle at 22 ± 2 °C with nesting material.

For the acute exercise bout, tibialis anterior muscles of PGC-1 α MKO mice and littermate control mice were collected 3 h after one bout of equal distance treadmill running (1.4 km) at 10° incline and 60% of their individual maximal running speed achieved by a graded treadmill running test⁹⁴.

For the ET intervention, mice were single-housed with or without access to in-cage running wheels from 8 to 20 weeks old. Running distance and duration were monitored by a regular cycle computer. PGC-1 α MKO mice tended to run less than lox/lox, thus running wheels of lox/lox mice were occasionally blocked to ensure equal running distance. On average, mice ran 25 km/week. The running wheels were blocked for all mice 24 h prior to euthanization and quadriceps muscle was harvested in the morning in the fed state.

AAV6 Vector construction and preparation. The AAV6 vector for SLIRP overexpression and ultra-purified eGFP control AAV6 virus were manufactured by VectorBuilder Inc. (Shenandoah, Texas, USA; AAV6SP(VB190219-1010jvy)-C).

Transfection of tibialis anterior muscle using rAAV6 vector. Viral particles were diluted in Gelfofusine (B. Braun, Germany) to a dosage of 5×10^9 vector genomes at a volume of 30 μ L per injection. For muscle-specific delivery of rAAV6 vectors, 12-week-old wildtype mice ($n = 6$) were placed under general anaesthesia (2% isofluorane in O₂), and injected intramuscularly with rAAV6:SLIRP in the TA muscle of one leg and control rAAV6:eGFP (empty vector) in the contralateral leg. Muscles were harvested 4 weeks after rAAV6 administration.

Time course of acute exercise. All mice were maintained under a 12:12 h light/dark photocycle at 22 ± 2 °C with nesting material. The female mice were group-housed. All mice received a rodent chow diet (Altromin no. 1324; Chr. Pedersen, Denmark) and water *ad libitum*.

Twelve-week old female C57BL/6J mice ($n = 8$ for each time point) were subjected to an acute exercise bout (1 h running, 60% of maximal running intensity, 15° incline). Quadriceps muscle was harvested from rested and exercised mice immediately after, 2 h, 6 h, and 24 h after the acute exercise bout.

SLIRP knockout mouse (*Slirp KO* mice). The generation of the model, quality, and specificity of the KO has been described previously¹⁸. Sperm of homozygous *Slirp* KO mice kindly provided by Nils-Göran Larsson and re-derived offspring was backcrossed to C57BL/6 N background in our own animal facilities.

All mice were maintained under a 12:12 h light/dark photocycle at 22 ± 2 °C with nesting material. The female mice were group-housed (except during the ET intervention), whereas the male mice were single-housed. All mice received a rodent chow diet (Altromin no. 1324; Chr. Pedersen, Denmark) and water *ad libitum*.

Mouse genotyping of *Slirp* KO and WT mice was performed as previously described¹⁹ using qPCR on DNA from ear punches with the following primers: WT; 5'-AGAAGGGAAT CCACAGGATA GGACA-3' and 5'-GCTTTATTCC TAGTGCCTGGC CTTGTT-3', KO; 5'-AGAAGGGAAT CCACAGGATA GGACA-3' and 5'-CGCCGTATAA TGTATGCTAT ACGAAGTT-3'.

10-week ET intervention in *Slirp* KO mice. For 10-week voluntary wheel-running exercise training interventions, 16–18-week-old *Slirp* KO and littermate mice were randomized into test groups with or without access to in-cage running wheels (Tecniplast activity cage, wheel diameter: 23 cm; Tecniplast, Buguggiate VA, Italy). The experimental design is schematically illustrated in Fig. 3A. Running distance was monitored by a regular cycle computer prior to the metabolic tests for 6 weeks. Running wheels were locked 12 h prior to terminal procedures to avoid effects of acute exercise bouts.

Body composition. Total, fat, and lean body mass was measured by nuclear magnetic resonance using an EchoMRI™ (USA).

Glucose tolerance test (GTT) and plasma insulin analysis. We subjected the *Slirp* KO and WT mice to a GTT at 7 weeks of the training intervention study (as illustrated in Fig. 3A). The GTT was executed after a 5 h fasting period (7:00 a.m.–12:00 p.m.). Resting blood samples were taken from the tail 30 min prior to the intraperitoneal injection of D-mono-glucose (2 g/kg body weight). Tail blood glucose was measured after 0, 20, 40, 60, and 90 min of injection.

To measure glucose-stimulated plasma insulin concentration at time-point (min) 0 and 20, tail vein blood samples were collected in a capillary-tube (50 µl), centrifuged at 14,200 g for 5 min at 4 °C, plasma collected and stored at –80 °C. Insulin concentration was determined in duplicates using the Ultra-Sensitive Mouse Insulin ELISA Kit (#80-INSTRU-E10; ALPCO Diagnostics) to the manufacturer's instructions. The incremental area under the curve (iAUC) from the basal blood glucose concentration was determined using the trapezoid rule.

Exercise capacity tests. *Slirp* KO and WT mice were acclimatized to the treadmill on 3 consecutive days by running at a speed of 0.16 m/s and incline of 10° for 5 min the first day and 10 min the following days. Prior to the running test and with a 1 h delay, 2 blood samples were drawn from the tail before the test for pre-exercise blood glucose and blood lactate measurements. Subsequently, the mice ran at 0.16 m/s for 5 min followed by a gradual increase in speed every minute with 0.02 m/s until exhaustion. Once the mouse reached its maximal running capacity, 2 blood samples were immediately drawn from the tail for post-exercise blood glucose and blood lactate measurements. The test was stopped when the mouse failed to keep up with the treadmill despite motivational efforts by the researcher.

In situ contraction. This protocol was described elsewhere⁹. The mice were anaesthetized by inhalation of 2% isoflurane during the entire procedure. Acupuncture needles (0.2 mm, TAI-CHI; B.C. Medical, Nykoebing SJ, Denmark) were inserted into both of the proximal and distal part of the mouse quadriceps femoris muscle of male 45–49 weeks old WT mice. The in situ contraction protocol consisted of nine

sets of contraction bouts of 1 min in duration, with a 30 s break between bouts. The contraction bouts consisted of 3 s of 10 V stimulations of pulses with a duration of 0.1 ms at a frequency of 100 Hz, repeated every 10 s. The contralateral leg served as a resting control. Two hours after the contraction, the mice were anaesthetized using 1:10 lidocaine:pentobarbital (6 mg of pentobarbital sodium 100 g⁻¹ body weight) by intraperitoneal injection and given a retro-orbital injection of 21.75 mg kg⁻¹ body weight puromycin (Calbiochem, San Diego, CA, USA) in saline. Exactly 15 min after puromycin injection, the mice were euthanized by cervical dislocation and Quad muscles were collected and snap frozen in liquid nitrogen.

TMRE staining in live fibers. Flexor digitorum brevis muscles (FDB) were dissected and then incubated for 2 h in serum-free α-MEM (22571-020, Gibco) containing 1.9 mg/ml collagenase type 1 from clostridium histolyticum (C0130, Sigma-Aldrich) and 1 mg/ml bovine serum albumin (9048-46-8, Sigma-Aldrich) at 37 °C on a rotator. After collagenase treatment, muscles were incubated in α-MEM containing 10% fetal bovine serum (26050-70, Gibco) and subjected to mechanical dissociation using fire-polished Pasteur pipettes. Single muscle fibers were seeded in 35x14mm glass-bottom microwell dishes (P35G-15-14-C, MatTek Corporation) coated with 4 µl of Engelbreth-Holm-Swarm murine sarcoma ECM gel (E1270, Merck). Muscle fibers were kept in α-MEM containing 5% fetal bovine serum in a cell incubator (37 °C, 5% CO₂) for at least 16 h prior to the experiments.

For determination of mitochondrial membrane potential (ΔΨ_{mitochondrial}) and mitochondrial network morphology, the fibers were incubated in 20 nM tetramethylrhodamine and ethyl ester (TMRE +, Life Technologies) dissolved in Krebs Ringer buffer (145 mM NaCl, 5 mM KCl, 1 mM CaCl₂, 1 mM MgCl₂, 5.6 mM glucose, 20 mM HEPES, pH 7.4) for 30 min before imaging. Confocal images were collected using a C-Apochromat ×40, 1.2 NA water immersion objective lens on an LSM 980 confocal microscope (Zeiss) driven Zeiss Zen Blue 3.

Mitochondrial network analysis was performed semi-automatically in ImageJ (National Institute of Health, USA). At least two nucleus-free regions per fiber were analyzed blindly. Before segmentation, the background was subtracted, and the pixels were averaged using a value of mean=2. The images were segmented, and particle analyses revealed the relative area of the TMRE+ signal compared to the total area (% mitochondrial area). The fragmentation index was calculated as the number of objects in relation to the total area covered by the dye. The ImageJ 'Red Hot' lookup table was used to visualize the images.

Transmission electron microscopy analysis. A small longitudinal section (<2 mm) of the red portion of the gastrocnemius muscle tissue was fixed by immersion 2% glutaraldehyde in 0.05 M Phosphatebuffer, pH 7.4 and stored at 4 °C. The samples were rinsed four times in 0.1 M sodium cacodylate buffer, pH 7.4, and post-fixed with 1% osmium tetroxide (OsO₄) and 1.5% potassium ferrocyanide [K₄Fe(CN)₆] in 0.1 M sodium cacodylate buffer, pH 7.4 for 90 min at 4 °C. The samples were then rinsed twice and dehydrated through a graded mixture of alcohol at 4–20 °C, infiltrated with graded mixtures of propylene oxide and Epon at 20 °C, and embedded in 100% Epon at 30 °C, as previously described (Nielsen et al., 2011). Longitudinally oriented sections, 60 nm thick, were obtained with a Leica UC7 ultramicrotome. The sections were contrasted with uranyl acetate and lead citrate, and subsequently examined and image recorded in a CM100 TEM (Philips, Eindhoven, The Netherlands) operated at 100 kV, and equipped with a Veleta camera and the iTEM software package (Olympus, Hamburg, Germany) at a resolution of 2048 × 2048 pixels.

A mean of eight fibers per sample (7–9) was included from the sectioned samples, and from each fiber, 24 images were obtained at $\times 13,500$ magnification. The imaging was performed in a randomized

systematic order including 12 images from the subsarcolemmal (SS) region, and 6 from both the superficial and central region of the intermyofibrillar (IMF) space. The Z-disc width was measured once on all IMF images and the mean from all fibers within one sample was calculated to determine the fiber type. The categorization of fiber types was based on previous reports from observations⁴⁸. The images were analyzed by two genotype-blinded investigators and all further analyses were performed by the same blinded investigator. The quantification of mitochondrial morphology was done using the Radius EM Imaging Software (Emsis GmbH, Radius 2.0).

Several measurements were included in this study: 1) Mitochondrial number: Total number of mitochondrial profiles (count). 2) Mitochondrial volume fraction: IMF mitochondrial volume is annotated as percentage of mitochondria covering the IMF space. 3) Damaged mitochondria: Mitochondria were categorized as damaged when they were swollen, vacuolated, or empty.

Mitochondrial respiration in gastrocnemius muscle. In a subset of mice, mitochondrial respiratory capacity was measured in permeabilized gastrocnemius skeletal muscle fibers as previously described⁹⁷. In brief, gastrocnemius muscle was rinsed from fat and connective tissue and separated into small fiber bundles. Fiber bundles were permeabilized with saponin (50 µg/ml) in BIOPS buffer for 30 min, followed by a 20 min wash in MiRO5 buffer on ice. Mitochondrial respiration was measured in duplicate under hyperoxic conditions at 37 °C using high resolution respirometry (Oxygraph-2k, Orophorus Instruments, Innsbruck, Austria). The following protocol was applied: Leak respiration was assessed by addition of malate (5 mM) and pyruvate (5 mM), followed by adding three different concentrations of ADP (0.01 mM, 0.25 mM and 5 mM; for the final concentration of ADP, 3 mM of magnesium (Mg) was added as well) to measure complex I linked respiratory capacity. 10 mM Glutamate was added to measure complex I linked respiratory capacity followed by 10 mM succinate to measure complex I + II linked respiratory capacity. Finally, 5 µM Antimycin A was added to inhibit complex III in the electron transport chain. Pooled data for both sexes are shown as no sex-specific differences were detected.

Contraction-stimulated fatty acid oxidation in isolated soleus muscles. Contraction-stimulated exogenous palmitate oxidation in isolated soleus muscle from *Slrp* KO and WT mice was measured as previously described⁹⁸. In brief, excised soleus muscles from mice anesthetized with pentobarbital were mounted at resting tension (~5 mN) in 15 ml vertical incubation chambers with a force transducer (Radnoti, Monrovia, CA) containing 30 °C carbonated (95% O₂ and 5% CO₂) Krebs-Henseleit Ringer buffer (KRB), pH = 7.4, supplemented with 5 mM glucose, 2% fatty acid-free BSA, and 0.5 mM palmitate. After ~20 min of pre-incubation, the incubation buffer was refreshed with KRB additionally containing [1-14 C]-palmitate (0.0044 MBq/ml; Amersham BioSciences, Buckinghamshire, U.K.). To seal the incubation chambers, mineral oil (Cat. No. M5904, Sigma-Aldrich) was added on top. Exogenous palmitate oxidation was measured simultaneously at rest and during 25 min contractions (18 trains/min, 0.6 s pulses, 30 Hz, 60 V). After incubation, incubation buffer and muscles were collected to determine the rate of palmitate oxidation as previously described^{97,99,100}. Palmitate oxidation was determined as CO₂ production (complete FA oxidation) and acid-soluble metabolites (representing incomplete FA oxidation). As no difference was observed in complete and incomplete FA oxidation between genotypes, palmitate oxidation is presented as a sum of these two forms.

Subcellular fractionations. The subcellular fractionation assay for frozen muscle was adapted^{44,45} and performed on ice or at 4 °C, where applicable. The frozen and pulverized muscle samples were homogenized for 2 min at 17.5 Hz using a TissueLyser II bead mill (QIAGEN,

USA) in cold isolation buffer solution, herein referred to as ISO buffer, containing 880 mM sucrose, 20 mM HEPES (pH 7.4), 50 mM NaCl, 5 mM MgCl₂, 5 mM EGTA, protease inhibitor and phosphatase inhibitor (cOmplete™ Protease Inhibitor and PhosStop™, Roche, Germany). The homogenate was then rotated end-over-end for 30 min and centrifuged at 1000 g for 10 min. The pellet was washed and centrifuged twice at 1000 g for 10 min in ISO buffer. The resulting pellet was used to prepare the nuclear fraction (not shown), while the supernatant was used to prepare the cytosolic and mitochondrial fractions.

For the cytosolic and mitochondrial fractions, the first supernatant fraction was centrifuged twice for 10 min at 1000 g. The resulting pellets were discarded, and the supernatant was centrifuged for 20 min at 20,000 g. From here the resulting supernatant and pellet were used to obtain the cytosolic and mitochondrial fractions, respectively.

For the cytosolic fraction, the supernatant was centrifuged twice for 20 min at 20,000 g and the resulting pellets were discarded. The final supernatant contained the cytosolic fraction.

For the mitochondrial fraction, the pellet was resuspended in 200 µl ISO buffer, centrifuged twice for 20 min at 20 000 g and the resulting supernatants were discarded. The resulting pellet was resuspended in 75 µL mitochondrial lysis buffer [50 mM Tris HCl (pH 6.8), 1 mM EDTA, 0.5% Triton X-100, and protease and phosphatase inhibitor] and rotated end-over-end for 20 min. The final suspension contained the mitochondrial fraction.

The total protein content of each subcellular fraction was determined colorimetrically, using the bicinchoninic acid method and bovine serum albumin (BSA) as a protein standard (Pierce BCA Protein Assay Kit, Thermo Fisher Scientific, Rockford, IL, USA). For subsequent immunoblotting, the same amount of protein was loaded onto each lane.

Lysate preparation and immunoblotting. Lysate preparation and immunoblotting of vastus lateralis muscles samples of HIIT in young, healthy men were performed as described by Hostrup et al.¹⁰¹, whereas lysate preparation and immunoblotting of vastus lateralis muscles of HIIT in individuals, who were lean, obese or T2D were performed as described by Kruse et al.¹⁰².

To preserve and assess PRDX3 dimer to monomer ratio, freshly harvested mouse gastrocnemius muscle tissue was incubated for 10 min in ice-cold 100 mM N-Ethylmaleimide (NEM) diluted in PBS. NEM was subsequently aspirated and the tissue homogenized for 1 min at 30 Hz using a TissueLyser II bead mill (QIAGEN, USA) in ice-cold homogenization buffer [10% glycerol, 1% NP-40, 20 mM sodium pyrophosphate, 150 mM NaCl, 50 mM Hepes (pH 7.5), 20 mM β-glycerophosphate, 10 mM NaF, 2 mM phenylmethylsulfonyl fluoride, 1 mM EDTA (pH 8.0), 1 mM EGTA (pH 8.0), 2 mM Na₃VO₄, leupeptin (10 µg ml⁻¹), aprotinin (10 µg ml⁻¹), and 3 mM benzamidine].

Lysate preparation and immunoblotting of all remaining mouse tissues and human vastus lateralis muscle samples of aerobic and strength ET in women⁶⁹, and resistance training in the young and elderly cohorts¹⁰³ were performed as previously described²⁵. Immunoblotting of the NEM-treated samples was performed under non-denaturing conditions. The primary antibodies used are listed in Supplementary Table 1.

Coomassie Brilliant Blue staining was used as a control to assess total protein loading and transfer efficiency¹⁰⁴ by quantifying the whole lane and for each sample set, a representative membrane from the immunoblotting is shown. The same Coomassie brilliant blue staining is presented for proteins analyzed when derived from the same sample set. Band densitometry was carried out using Image Lab (version 6.0.1). For each set of samples, a standard curve was loaded to ensure quantification within the linear range for each protein probed for. Uncropped and unprocessed scans of all blots are included in the Source Data file.

RNA extraction and RT-qPCR. Figures 1J, 4F: RNA was extracted from ~20 mg of pulverized whole mouse gastrocnemius muscle using TRIzol™ reagent (Invitrogen) following the manufacturer's instructions (tissue homogenization was performed using the MP Bio lysis system) and treated with the TURBO DNA-free™ Kit (Ambion) to remove contaminating DNA. For RT-qPCR expression analysis, cDNA was reversed transcribed from 0.85 µg total RNA using the High-Capacity cDNA Reverse Transcription Kit (Applied Biosystems) in the presence of RNase Block (Agilent). The qPCR was performed in a QuantStudio 6 Flex Real-Time PCR System (Life Technologies), using TaqMan™ Universal Master Mix II, with UNG (Applied Biosystems) to quantify mitochondrial transcripts (mitochondrial-rRNAs and mt-mRNAs). The gene expression levels were determined using the $\Delta\Delta Ct$ method, comparing the Ct values of mitochondrial transcripts to that of the beta-actin reference gene for normalization.

Figure 2A, C-E: Total RNA was extracted from pulverized quadriceps muscle using an adapted guanidinium thiocyanate-phenol-chloroform extraction method. Reverse transcription to cDNA was performed as previously described⁵¹. Real-time qPCR was performed in triplicate for 2A, C, D and duplicate for 2E with QuantStudio 7 Flex Real-Time PCR System (Applied Biosystems, Waltham, MA). Cycle threshold (Ct) was converted to a relative amount using a standard curve derived from a serial dilution of a representative pooled samples run together with the samples of interest. Beta-actin or Hprt mRNA was used for normalization of target mRNA levels.

Figure 6D: Total RNA extraction from vastus lateralis muscle and reverse transcription to cDNA was performed as previously described⁷⁰. The qPCR was performed in a QuantStudio 6 Flex Real-Time PCR System (Life Technologies), using TaqMan™ Universal Master Mix II (Applied Biosystems) to quantify mt-mRNAs. The gene expression levels were determined using the $\Delta\Delta Ct$ method, comparing the Ct values of mitochondrial transcripts to that of the 18S rRNA reference gene for normalization.

Figure 6G: Total RNA was extracted from skeletal muscle biopsies using TRI Reagent (Sigma-Aldrich) following the manufacturer's instructions. cDNA was reversed transcribed using the High-Capacity cDNA Reverse Transcription Kit (Applied Biosystems), while the qPCR was performed on an Aria Mx (Agilent) using a TaqMan™ Universal Master Mix II (Applied Biosystems). The gene expression levels were determined using the $\Delta\Delta Ct$ method with the mRNA levels being normalized to the geometric mean of *PPIA* and *B2M*.

Primers or Taqman probes or Taqman expression assays used for mRNA levels measured in Figs. 2, 4 and 6 are shown in Supplementary Table 2.

DNA isolation and mtDNA quantification. Total DNA was extracted from ~20 mg mouse gastrocnemius muscle using the Dneasy Blood and Tissue Kit (Qiagen) according to the manufacturer's instructions and treated with RNase A. Levels of mtDNA were measured by qPCR using 2.5 ng of DNA in a QuantStudio 6 Flex Real-Time PCR System using TaqMan™ Universal Master Mix II, with UNG. The mt-Nd1 and mt-Nd6/Nd5 TaqMan gene expression assays were used. 18S rRNA was used for normalization.

Aerobic and strength ET intervention in healthy young women. A detailed description of the study participants, research design and methods has been previously published^{69,70}. In the present study, we included vastus lateralis muscle lysate for immunoblotting obtained from 9 healthy young women (age, 33 ± 6 years; body mass index (BMI), $23.2 \pm 2.6 \text{ kg m}^{-2}$) before and after 14-week of aerobic and strength exercise training.

High-intensity interval training intervention in healthy young men. A detailed description of the study participants, research design and methods has been previously published⁷². In the present study, we

included vastus lateralis muscle lysate for immunoblotting obtained from 6 healthy young men before and after 6-week HIIT training.

Progressive resistance exercise training in male young and older individuals. A detailed description of the study participants, research design and methods has been previously published⁷⁰. The original study reported no additive effect of vitamin D intake during the 12 weeks of resistance exercise training on muscle hypertrophy or muscle strength^{69,70}. Accordingly, in the present study, samples from young or older participants were considered as one group, irrespective of vitamin D intake. We included vastus lateralis muscle samples (~10 mg wet weight) for immunoblotting obtained from a subset of the original sample set due to lack of sample material. For the young participants, we included 10 samples before and 6 samples after resistance exercise training. For the older participants we included 11 before and 9 samples after resistance exercise training.

High-intensity interval training in middle-aged male individuals, who were lean, obese or obese with type 2 diabetes. A detailed description of the study participants, eligibility criteria, research design and methods has been previously published⁷¹. In brief, 15 middle-aged men with T2D and obesity, 15 age- and BMI-matched glucose-tolerant men with obesity, and 18 age-matched glucose-tolerant lean men were recruited. All participants, except four (two men with T2D and obesity and two lean men), completed the study. The training protocol consisted of 8-weeks with three weekly training sessions consisting of supervised HIIT in combination with biking and rowing. HIIT-sessions consisted of 5×1 min exercise blocks interspersed with 1 min rest, and shifted between blocks on cycle and rowing ergometers. The volume was increased from two to five blocks during the 8 weeks. In the present study, we included vastus lateralis muscle samples that were obtained 4–5 days after the last HIIT session but 48 h after the last physical activity (a VO_2 max test). The number of samples included for immunoblotting were as follows: 16 before and after HIIT from lean glucose-tolerant men, 15 before and after HIIT from glucose-tolerant men with obesity, and 13 before and after HIIT from men with T2D and obesity.

Graphical illustrations. Graphical illustrations were created in ©BioRender - biorender.com, as indicated in the figure legends.

Statistical methods

Results are presented as mean \pm SEM with individual values shown, when feasible. Statistical differences were analyzed by ordinary one-way ANOVA, repeated/ordinary two-way ANOVA, or Log-rank (Mantel-Cox) test, and Mann-Whitney test as applicable. Dunnett's multiple comparisons test or Šídák's multiple comparisons test were used to evaluate significant interactions in ANOVAs. Percentage change analysis was performed by Mean difference and 95% CI of difference calculated by Uncorrected Fisher's LSD. Pearson correlation coefficients were calculated. As statistical tests varied according to the dataset being analyzed, the respective tests utilized are specified within the figure legends. $0.05 \leq p < 0.1$ were considered a tendency and p values < 0.05 were considered significant.

Reporting summary

Further information on research design is available in the Nature Portfolio Reporting Summary linked to this article.

Data availability

The authors declare that all data supporting the findings of this study are available within the paper (and its supplementary information files). Source data are provided with this paper.

References

1. Romanello, V. & Sandri, M. The connection between the dynamic remodeling of the mitochondrial network and the regulation of muscle mass. *Cell Mol. Life Sci.* **78**, 1305–1328 (2021).
2. Distefano, G. et al. Physical activity unveils the relationship between mitochondrial energetics, muscle quality, and physical function in older adults. *J. Cachexia Sarcopenia Muscle* **9**, 279–294 (2018).
3. Gonzalez-Freire, M. et al. Reconsidering the role of mitochondria in aging. *J. Gerontol. A Biol. Sci. Med Sci.* **70**, 1334–1342 (2015).
4. Janssen, I., Heymsfield, S. B. & Ross, R. Low relative skeletal muscle mass (sarcopenia) in older persons is associated with functional impairment and physical disability. *J. Am. Geriatr. Soc.* **50**, 889–896 (2002).
5. Short, K. R. et al. Decline in skeletal muscle mitochondrial function with aging in humans. *Proc. Natl Acad. Sci. USA* **102**, 5618–5623 (2005).
6. Haines, M. S., Leong, A., Porneala, B. C., Meigs, J. B. & Miller, K. K. Association between muscle mass and diabetes prevalence independent of body fat distribution in adults under 50 years old. *Nutr. Diab.* **12**, 29 (2022).
7. Sugimoto, K. et al. Hyperglycemia in non-obese patients with type 2 diabetes is associated with low muscle mass: The Multicenter Study for Clarifying Evidence for Sarcopenia in Patients with Diabetes Mellitus. *J. Diab. Investig.* **10**, 1471–1479 (2019).
8. Yoon, J. W. et al. Hyperglycemia is associated with impaired muscle quality in older men with diabetes: the korean longitudinal study on health and aging. *Diab. Metab. J.* **40**, 140–146 (2016).
9. Ebhardt, H. A. et al. Comprehensive proteome analysis of human skeletal muscle in cachexia and sarcopenia: a pilot study. *J. Cachexia Sarcopenia Muscle* **8**, 567–582 (2017).
10. Romanello, V. & Sandri, M. Mitochondrial quality control and muscle mass maintenance. *Front Physiol.* **6**, 422 (2015).
11. Safdar, A. et al. Endurance exercise rescues progeroid aging and induces systemic mitochondrial rejuvenation in mtDNA mutator mice. *Proc. Natl Acad. Sci. USA* **108**, 4135–4140 (2011).
12. Pedersen, B. K. & Saltin, B. Exercise as medicine - evidence for prescribing exercise as therapy in 26 different chronic diseases. *Scand. J. Med Sci. Sports* **25**, 1–72 (2015).
13. Adhiketty, P. J., Taivassalo, T., Haller, R. G., Walkinshaw, D. R. & Hood, D. A. The effect of training on the expression of mitochondrial biogenesis- and apoptosis-related proteins in skeletal muscle of patients with mtDNA defects. *Am. J. Physiol. Endocrinol. Metab.* **293**, E672–E680 (2007).
14. Sylow, L., Kleinert, M., Richter, E. A. & Jensen, T. E. Exercise-stimulated glucose uptake - regulation and implications for glycaemic control. *Nat. Rev. Endocrinol.* **13**, 133–148 (2017).
15. Boengler, K., Heusch, G. & Schulz, R. Nuclear-encoded mitochondrial proteins and their role in cardioprotection. *Biochim Biophys. Acta* **1813**, 1286–1294 (2011).
16. Couvillion, M. T., Soto, I. C., Shipkovenska, G. & Churchman, L. S. Synchronized mitochondrial and cytosolic translation programs. *Nature* **533**, 499–503 (2016).
17. Sasarman, F. et al. LRPPRC and SLIRP interact in a ribonucleoprotein complex that regulates posttranscriptional gene expression in mitochondria. *Mol. Biol. Cell* **21**, 1315–1323 (2010).
18. Lagouge, M. et al. SLIRP Regulates the Rate of Mitochondrial Protein Synthesis and Protects LRPPRC from Degradation. *PLoS Genet* **11**, e1005423 (2015).
19. Ruzzene, B. et al. LRPPRC is necessary for polyadenylation and coordination of translation of mitochondrial mRNAs. *EMBO J.* **31**, 443–456 (2012).
20. Chujo, T. et al. LRPPRC/SLIRP suppresses PNase-mediated mRNA decay and promotes polyadenylation in human mitochondria. *Nucleic Acids Res* **40**, 8033–8047 (2012).
21. Baughman, J. M. et al. A computational screen for regulators of oxidative phosphorylation implicates SLIRP in mitochondrial RNA homeostasis. *PLoS Genet* **5**, e1000590 (2009).
22. Hatchell, E. C. et al. SLIRP, a small SRA binding protein, is a nuclear receptor corepressor. *Mol. Cell* **22**, 657–668 (2006).
23. Cooper, M. P. et al. Defects in energy homeostasis in Leigh syndrome French Canadian variant through PGC-1alpha/LRP130 complex. *Genes Dev.* **20**, 2996–3009 (2006).
24. Holloszy, J. O. Biochemical adaptations in muscle. Effects of exercise on mitochondrial oxygen uptake and respiratory enzyme activity in skeletal muscle. *J. Biol. Chem.* **242**, 2278–2282 (1967).
25. Kleinert, M. et al. Quantitative proteomic characterization of cellular pathways associated with altered insulin sensitivity in skeletal muscle following high-fat diet feeding and exercise training. *Sci. Rep.* **8**, 10723 (2018).
26. Brand, A. H. & Perrimon, N. Targeted gene expression as a means of altering cell fates and generating dominant phenotypes. *Development* **118**, 401–415 (1993).
27. Baggio, F. et al. Drosophila melanogaster LRPPRC2 is involved in coordination of mitochondrial translation. *Nucleic Acids Res* **42**, 13920–13938 (2014).
28. Bratic, A. et al. The bicoid stability factor controls polyadenylation and expression of specific mitochondrial mRNAs in Drosophila melanogaster. *PLoS Genet* **7**, e1002324 (2011).
29. Matsushima, Y. et al. Drosophila protease ClpXP specifically degrades DmLRPPRC1 controlling mitochondrial mRNA and translation. *Sci. Rep.* **7**, 8315 (2017).
30. Inagaki, H. K., Kamikouchi, A. & Ito, K. Methods for quantifying simple gravity sensing in Drosophila melanogaster. *Nat. Protoc.* **5**, 20–25 (2010).
31. Baar, K. et al. Adaptations of skeletal muscle to exercise: rapid increase in the transcriptional coactivator PGC-1. *FASEB J.* **16**, 1879–1886 (2002).
32. Chinsomboon, J. et al. The transcriptional coactivator PGC-1alpha mediates exercise-induced angiogenesis in skeletal muscle. *Proc. Natl Acad. Sci. USA* **106**, 21401–21406 (2009).
33. Pilegaard, H., Saltin, B. & Neufer, P. D. Exercise induces transient transcriptional activation of the PGC-1alpha gene in human skeletal muscle. *J. Physiol.* **546**, 851–858 (2003).
34. Kjobsted, R. et al. Intact regulation of the ampk signaling network in response to exercise and insulin in skeletal muscle of male patients with type 2 diabetes: illumination of ampk activation in recovery from exercise. *Diabetes* **65**, 1219–1230 (2016).
35. Halling, J. F. & Pilegaard, H. PGC-1alpha-mediated regulation of mitochondrial function and physiological implications. *Appl Physiol. Nutr. Metab.* **45**, 927–936 (2020).
36. Ruas, J. L. et al. A PGC-1alpha isoform induced by resistance training regulates skeletal muscle hypertrophy. *Cell* **151**, 1319–1331 (2012).
37. Jannig, P. R., Dumesic, P. A., Spiegelman, B. M. & Ruas, J. L. SnapShot: Regulation and biology of PGC-1alpha. *Cell* **185**, 1444–1444.e1441 (2022).
38. Lin, J. et al. Transcriptional co-activator PGC-1 alpha drives the formation of slow-twitch muscle fibres. *Nature* **418**, 797–801 (2002).
39. Arany, Z. PGC-1 coactivators and skeletal muscle adaptations in health and disease. *Curr. Opin. Genet Dev.* **18**, 426–434 (2008).
40. Handschin, C. et al. Abnormal glucose homeostasis in skeletal muscle-specific PGC-1alpha knockout mice reveals skeletal muscle-pancreatic beta cell crosstalk. *J. Clin. Invest.* **117**, 3463–3474 (2007).
41. Miller, B. F., Konopka, A. R. & Hamilton, K. L. The rigorous study of exercise adaptations: why mRNA might not be enough. *J. Appl Physiol.* (1985) **121**, 594–596 (2016).

42. Robinson, M. M. et al. Enhanced protein translation underlies improved metabolic and physical adaptations to different exercise training modes in young and old humans. *Cell Metab.* **25**, 581–592 (2017).
43. Liu, Y., Beyer, A. & Aebersold, R. On the dependency of cellular protein levels on mRNA abundance. *Cell* **165**, 535–550 (2016).
44. Dias, P. R. F., Gandra, P. G., Brenzikofer, R. & Macedo, D. V. Subcellular fractionation of frozen skeletal muscle samples. *Biochem Cell Biol.* **98**, 293–298 (2020).
45. Dimauro, I., Pearson, T., Caporossi, D. & Jackson, M. J. A simple protocol for the subcellular fractionation of skeletal muscle cells and tissue. *BMC Res Notes* **5**, 513 (2012).
46. Richter, E. A. & Ruderman, N. B. AMPK and the biochemistry of exercise: implications for human health and disease. *Biochem J.* **418**, 261–275 (2009).
47. Fentz, J. et al. AMPK α is critical for enhancing skeletal muscle fatty acid utilization during in vivo exercise in mice. *FASEB J.* **29**, 1725–1738 (2015).
48. Lantier, L. et al. AMPK controls exercise endurance, mitochondrial oxidative capacity, and skeletal muscle integrity. *FASEB J.* **28**, 3211–3224 (2014).
49. Handschin, C. et al. Skeletal muscle fiber-type switching, exercise intolerance, and myopathy in PGC-1 α muscle-specific knockout animals. *J. Biol. Chem.* **282**, 30014–30021 (2007).
50. Raun, S. H. et al. Housing temperature influences exercise training adaptations in mice. *Nat. Commun.* **11**, 1560 (2020).
51. Brandt, N. et al. The impact of exercise training and resveratrol supplementation on gut microbiota composition in high-fat diet fed mice. *Physiol. Rep.* **6**, e13881 (2018).
52. Wojtaszewski, J. F. & Richter, E. A. Effects of acute exercise and training on insulin action and sensitivity: focus on molecular mechanisms in muscle. *Essays Biochem.* **42**, 31–46 (2006).
53. Memme, J. M. & Hood, D. A. Molecular Basis for the Therapeutic Effects of Exercise on Mitochondrial Defects. *Front Physiol.* **11**, 615038 (2020).
54. Carter, H. N., Pauly, M., Tryon, L. D. & Hood, D. A. Effect of contractile activity on PGC-1 α transcription in young and aged skeletal muscle. *J. Appl Physiol.* (1985) **124**, 1605–1615 (2018).
55. Lanza, I. R. et al. Endurance exercise as a countermeasure for aging. *Diabetes* **57**, 2933–2942 (2008).
56. Schaefer, P. M. et al. Mitochondrial mutations alter endurance exercise response and determinants in mice. *Proc. Natl Acad. Sci. USA* **119**, e2200549119 (2022).
57. Yoshida, Y. et al. Exercise- and training-induced upregulation of skeletal muscle fatty acid oxidation are not solely dependent on mitochondrial machinery and biogenesis. *J. Physiol.* **591**, 4415–4426 (2013).
58. Spahr, H. et al. SLIRP stabilizes LRPPRC via an RRM-PPR protein interface. *Nucleic Acids Res* **44**, 6868–6882 (2016).
59. Filograna, R., Mennuni, M., Alsina, D. & Larsson, N. G. Mitochondrial DNA copy number in human disease: the more the better? *FEBS Lett.* **595**, 976–1002 (2021).
60. Houtkooper, R. H. et al. Mitonuclear protein imbalance as a conserved longevity mechanism. *Nature* **497**, 451–457 (2013).
61. Larsen, S. et al. Biomarkers of mitochondrial content in skeletal muscle of healthy young human subjects. *J. Physiol.* **590**, 3349–3360 (2012).
62. Halling, J. F., Ringholm, S., Olesen, J., Prats, C. & Pilegaard, H. Exercise training protects against aging-induced mitochondrial fragmentation in mouse skeletal muscle in a PGC-1 α dependent manner. *Exp. Gerontol.* **96**, 1–6 (2017).
63. Metodiev, M. D. et al. Methylation of 12S rRNA is necessary for in vivo stability of the small subunit of the mammalian mitochondrial ribosome. *Cell Metab.* **9**, 386–397 (2009).
64. Yang, Y. et al. NAD $^{+}$ -dependent deacetylase SIRT3 regulates mitochondrial protein synthesis by deacetylation of the ribosomal protein MRPL10. *J. Biol. Chem.* **285**, 7417–7429 (2010).
65. Costa-Mattioli, M. & Walter, P. The integrated stress response: From mechanism to disease. *Science* **368**, eaat5314 (2020).
66. Szczepanowska, K. & Trifunovic, A. Mitochondrial matrix proteases: quality control and beyond. *FEBS J.* **289**, 7128–7146 (2022).
67. Cox, A. G., Winterbourn, C. C. & Hampton, M. B. Mitochondrial peroxiredoxin involvement in antioxidant defence and redox signalling. *Biochem J.* **425**, 313–325 (2009).
68. Lee, K. P. et al. Peroxiredoxin 3 has a crucial role in the contractile function of skeletal muscle by regulating mitochondrial homeostasis. *Free Radic. Biol. Med.* **77**, 298–306 (2014).
69. Hansen, S. L. et al. Mechanisms Underlying Absent Training-Induced Improvement in Insulin Action in Lean, Hyperandrogenic Women With Polycystic Ovary Syndrome. *Diabetes* **69**, 2267–2280 (2020).
70. Agergaard, J. et al. Does vitamin-D intake during resistance training improve the skeletal muscle hypertrophic and strength response in young and elderly men? - a randomized controlled trial. *Nutr. Metab. (Lond.)* **12**, 32 (2015).
71. Petersen, M. H. et al. High-intensity interval training combining rowing and cycling efficiently improves insulin sensitivity, body composition and VO (2) max in men with obesity and type 2 diabetes. *Front Endocrinol. (Lausanne)* **13**, 1032235 (2022).
72. Hostrup, M. et al. High-Intensity Training Represses FXYD5 and Glycosylates Na,K-ATPase in Type II Muscle Fibres, Which Are Linked with Improved Muscle K $(+)$ Handling and Performance. *Int. J. Mol. Sci.* **24**, 5587 (2023).
73. Hey-Mogensen, M. et al. Effect of physical training on mitochondrial respiration and reactive oxygen species release in skeletal muscle in patients with obesity and type 2 diabetes. *Diabetologia* **53**, 1976–1985 (2010).
74. Phielix, E., Meex, R., Moonen-Kornips, E., Hesselink, M. K. & Schrauwen, P. Exercise training increases mitochondrial content and ex vivo mitochondrial function similarly in patients with type 2 diabetes and in control individuals. *Diabetologia* **53**, 1714–1721 (2010).
75. Karakelides, H., Irving, B. A., Short, K. R., O'Brien, P. & Nair, K. S. Age, obesity, and sex effects on insulin sensitivity and skeletal muscle mitochondrial function. *Diabetes* **59**, 89–97 (2010).
76. Schwanhausser, B. et al. Global quantification of mammalian gene expression control. *Nature* **473**, 337–342 (2011).
77. Gineste, C. et al. Enzymatically dissociated muscle fibers display rapid dedifferentiation and impaired mitochondrial calcium control. *iScience* **25**, 105654 (2022).
78. Copeland, J. M. et al. Extension of *Drosophila* life span by RNAi of the mitochondrial respiratory chain. *Curr. Biol.* **19**, 1591–1598 (2009).
79. Dell'agnello, C. et al. Increased longevity and refractoriness to Ca $(2+)$ -dependent neurodegeneration in *Surf1* knockout mice. *Hum. Mol. Genet.* **16**, 431–444 (2007).
80. Dillin, A. et al. Rates of behavior and aging specified by mitochondrial function during development. *Science* **298**, 2398–2401 (2002).
81. Rossignol, R. et al. Mitochondrial threshold effects. *Biochem J.* **370**, 751–762 (2003).
82. Hwang, A. B., Jeong, D. E. & Lee, S. J. Mitochondria and organismal longevity. *Curr. Genomics* **13**, 519–532 (2012).
83. Xu, C. et al. Genetic inhibition of an ATP synthase subunit extends lifespan in *C. elegans*. *Sci. Rep.* **8**, 14836 (2018).
84. Liu, X. et al. Evolutionary conservation of the clk-1-dependent mechanism of longevity: loss of mclk1 increases cellular fitness and lifespan in mice. *Genes Dev.* **19**, 2424–2434 (2005).

85. Rubalcava-Gracia, D. et al. LRPPRC and SLIRP synergize to maintain sufficient and orderly mammalian mitochondrial translation. *Nucleic Acids Res.* **52**, 11266–11282 (2024).
86. Leick, L. et al. PGC-1alpha is not mandatory for exercise- and training-induced adaptive gene responses in mouse skeletal muscle. *Am. J. Physiol. Endocrinol. Metab.* **294**, E463–E474 (2008).
87. Larsen, S., Skaaby, S., Helge, J. W. & Dela, F. Effects of exercise training on mitochondrial function in patients with type 2 diabetes. *World J. Diab.* **5**, 482–492 (2014).
88. Sylow, L., Tokarz, V. L., Richter, E. A. & Klip, A. The many actions of insulin in skeletal muscle, the paramount tissue determining glycemia. *Cell Metab.* **33**, 758–780 (2021).
89. Richter, E. A., Sylow, L. & Hargreaves, M. Interactions between insulin and exercise. *Biochem J.* **478**, 3827–3846 (2021).
90. Cartee, G. D. Sexual Dimorphic Effects of Exercise Training on Subcutaneous White Adipose Tissue of Mice. *Diabetes* **70**, 1242–1243 (2021).
91. Holcomb, L. E. et al. Sex differences in endurance exercise capacity and skeletal muscle lipid metabolism in mice. *Physiol. Rep.* **10**, e15174 (2022).
92. Rooyackers, O. E., Adey, D. B., Ades, P. A. & Nair, K. S. Effect of age on in vivo rates of mitochondrial protein synthesis in human skeletal muscle. *Proc. Natl Acad. Sci. USA* **93**, 15364–15369 (1996).
93. Ganetzky, B. & Flanagan, J. R. On the relationship between senescence and age-related changes in two wild-type strains of *Drosophila melanogaster*. *Exp. Gerontol.* **13**, 189–196 (1978).
94. Correia, J. C. et al. Muscle-secreted neurturin couples myofiber oxidative metabolism and slow motor neuron identity. *Cell Metab.* **33**, 2215–2230.e2218 (2021).
95. Geng, T. et al. PGC-1alpha plays a functional role in exercise-induced mitochondrial biogenesis and angiogenesis but not fiber-type transformation in mouse skeletal muscle. *Am. J. Physiol. Cell Physiol.* **298**, C572–C579 (2010).
96. Knudsen, J. R. et al. Contraction-regulated mTORC1 and protein synthesis: Influence of AMPK and glycogen. *J. Physiol.* **598**, 2637–2649 (2020).
97. Jeppesen, J. et al. LKB1 regulates lipid oxidation during exercise independently of AMPK. *Diabetes* **62**, 1490–1499 (2013).
98. Eisenberg, B. R. Quantitative ultrastructure of mammalian skeletal muscle, in *Handbook of Physiology, Skeletal Muscle*. (eds. L.D. Peachey, R. H. Adrian & S. R. Geiger) p. 73–112 (American Physiological Society, Bethesda, MD; 1983).
99. Pesta, D. & Gnaiger, E. High-resolution respirometry: OXPHOS protocols for human cells and permeabilized fibers from small biopsies of human muscle. *Methods Mol. Biol.* **810**, 25–58 (2012).
100. Dzamko, N. et al. AMPK-independent pathways regulate skeletal muscle fatty acid oxidation. *J. Physiol.* **586**, 5819–5831 (2008).
101. Hostrup, M. et al. High-intensity interval training remodels the proteome and acetylome of human skeletal muscle. *Elife* **11**, e69802 (2022).
102. Kruse, R. et al. Intact initiation of autophagy and mitochondrial fission by acute exercise in skeletal muscle of patients with Type 2 diabetes. *Clin. Sci. (Lond.)* **131**, 37–47 (2017).
103. Kruse, R. et al. Effect of long-term testosterone therapy on molecular regulators of skeletal muscle mass and fibre-type distribution in aging men with subnormal testosterone. *Metabolism* **112**, 154347 (2020).
104. Welinder, C. & Ekblad, L. Coomassie staining as loading control in Western blot analysis. *J. Proteome Res.* **10**, 1416–1419 (2011).
105. Lord, S. J., Velle, K. B., Mullins, R. D. & Fritz-Laylin, L. K. SuperPlots: Communicating reproducibility and variability in cell biology. *J. Cell Biol.* **219**, e202001064 (2020).

Acknowledgements

We acknowledge the technical assistance of Betina Bolmgren and Irene Nielsen, Martin Thomassen, and Roberto Meneses-Valdes (Department of Nutrition, Exercise and Sports, Faculty of Science, University of Copenhagen, Denmark), Anja Jokipii-Utzon (Institute of Sports Medicine, Bispebjerg Hospital, Copenhagen, Denmark), Michala Carlsson and Katrine Brantbjerg Mosegaard (Department of Biomedical Sciences, University of Copenhagen, Denmark). We thank Vivian Shang for her assistance with the *Drosophila* experiments (Charles Perkins Centre, The University of Sydney, Australia). We acknowledge Cristiano di Benedetto for preparing muscle samples for TEM analysis (Core Facility for Integrated Microscopy, Faculty of Health and Medical Sciences, University of Copenhagen, Denmark). We thank Professor Rudolf J. Wiesner for generously providing us with the MRPL12, MRPS18B, MRPS35 and YME1L1 antibodies (Institute of Vegetative Physiology, Faculty of Medicine and University Hospital Cologne, Cologne, Germany). The study was supported by the Novo Nordisk Foundation (grant NNF16OC0023418, NNF18OC0032082, and NNF20OC0063577 to L.S.; grant NNF22OC0074110 to A.M.F.), by Independent Research Fund Denmark to L.S. (#0169-00013B), by the European Union's Horizon 2020 research and innovation programme (Marie Skłodowska-Curie grant agreement No 801199 to T.C.P.P. and E.A.R.), grants by Danish Council for Independent Research - Medical Sciences (4181-00078) and the Augustinus Foundation to H.P. and grants from the Independent Research Fund Denmark (2030-00007 A) and Lundbeck Foundation (R380-2021-1451) to S.H.R.

Author contributions

T.C.P.P.: Conceptualization, Methodology, Validation, Formal analysis, Investigation, Writing - Original Draft, Visualization, Project administration, Funding acquisition; S.H.R.: Conceptualization; Investigation, Writing - Review & Editing; E.H.: Methodology, Investigation, Writing - Review & Editing; C.H.-O.: Methodology, Investigation, Writing - Review & Editing; D.R.-G.: Methodology, Investigation, Writing - Review & Editing; E.F.: Methodology, Investigation, Writing - Review & Editing; A.M.F.: Methodology, Investigation, Writing - Review & Editing; P.J.: Methodology, Investigation, Writing - Review & Editing; N.R.A.: Investigation, Writing - Review & Editing; R.K.: Investigation, Writing - Review & Editing; M.S.A.: Investigation, Writing - Review & Editing; A.I.: Investigation, Writing - Review & Editing; J.F.H.: Resources, Writing - Review & Editing; S.R.: Resources, Writing - Review & Editing; E.J.N.: Methodology, Writing - Review & Editing; S.H.: Resources, Writing - Review & Editing; A.K.L.: Resources, Writing - Review & Editing; M.H.P.: Resources, Writing - Review & Editing; M.E.de.A.: Resources, Writing - Review & Editing; T.E.J.: Resources, Writing - Review & Editing; B.K.: Resources, Writing - Review & Editing; M.H.: Resources, Writing - Review & Editing; S.L.N.: Methodology, Investigation, Writing - Review & Editing; N.Ø.: Resources, Writing - Review & Editing; K.H.: Resources, Writing - Review & Editing; P.S.: Methodology, Investigation, Resources, Writing - Review & Editing; M.K.: Resources, Writing - Review & Editing; J.R.: Resources, Writing - Review & Editing; A.T.: Resources, Writing - Review & Editing; J.W.: Resources, Writing - Review & Editing; J.N.: Methodology, Investigation, Writing - Review & Editing; K.Q.: Resources, Writing - Review & Editing; H.P.: Resources, Writing - Review & Editing; E.A.R.: Resources, Investigation, Writing - Review & Editing, Supervision, Funding acquisition; L.S.: Conceptualization, Methodology, Validation, Formal analysis, Investigation, Writing - Original Draft, Project administration, Supervision, Funding acquisition.

Competing interests

Since the study concluded, Solvejg Hansen, Jens Frey Halling and Anders Krogh Lemminger have become employees and shareholders of Novo Nordisk A/S, Denmark. The remaining authors declare no competing interests.

Additional information

Supplementary information The online version contains supplementary material available at
<https://doi.org/10.1038/s41467-024-54183-4>.

Correspondence and requests for materials should be addressed to Lykke Sylow.

Peer review information *Nature Communications* thanks the anonymous reviewers for their contribution to the peer review of this work. A peer review file is available.

Reprints and permissions information is available at
<http://www.nature.com/reprints>

Publisher's note Springer Nature remains neutral with regard to jurisdictional claims in published maps and institutional affiliations.

Open Access This article is licensed under a Creative Commons Attribution-NonCommercial-NoDerivatives 4.0 International License, which permits any non-commercial use, sharing, distribution and reproduction in any medium or format, as long as you give appropriate credit to the original author(s) and the source, provide a link to the Creative Commons licence, and indicate if you modified the licensed material. You do not have permission under this licence to share adapted material derived from this article or parts of it. The images or other third party material in this article are included in the article's Creative Commons licence, unless indicated otherwise in a credit line to the material. If material is not included in the article's Creative Commons licence and your intended use is not permitted by statutory regulation or exceeds the permitted use, you will need to obtain permission directly from the copyright holder. To view a copy of this licence, visit <http://creativecommons.org/licenses/by-nc-nd/4.0/>.

© The Author(s) 2024

Tang Cam Phung Pham ^{1,2}, Steffen Henning Raun², Essi Havula³, Carlos Henriquez-Olguín  ^{1,4}, Diana Rubalcava-Gracia  ⁵, Emma Frank², Andreas Mæchel Fritzen  ^{1,2}, Paulo R. Jannig  ⁶, Nicoline Resen Andersen¹, Rikke Kruse⁷, Mona Sadek Ali², Andrea Irazoki  ², Jens Frey Halling⁸, Stine Ringholm⁸, Elise J. Needham⁹, Solvejg Hansen¹, Anders Krogh Lemminger¹, Peter Schjerling  ^{10,11}, Maria Houborg Petersen  ⁷, Martin Eisemann de Almeida  ^{7,12}, Thomas Elbenhardt Jensen  ¹, Bente Kiens  ¹, Morten Hostrup  ¹, Steen Larsen  ^{2,10,11,13}, Niels Ørtenblad  ¹², Kurt Højlund  ^{7,14}, Michael Kjær  ^{10,11}, Jorge L. Ruas⁶, Aleksandra Trifunovic  ¹⁵, Jørgen Frank Pind Wojtaszewski  ¹, Joachim Nielsen  ¹², Klaus Qvortrup  ², Henriette Pilegaard  ⁸, Erik Arne Richter  ¹ & Lykke Sylow  ^{1,2} 

¹Department of Nutrition, Exercise and Sports, Faculty of Science, University of Copenhagen, Copenhagen, Denmark. ²Department of Biomedical Sciences, Faculty of Health and Medical Sciences, University of Copenhagen, Copenhagen, Denmark. ³Stem Cells and Metabolism Research Program, Faculty of Medicine, University of Helsinki, Helsinki, Finland. ⁴Exercise Science Laboratory, Faculty of Medicine, Universidad Finis Terrae, Av. Pedro de Valdivia 1509, Santiago, Chile. ⁵Division of Molecular Metabolism, Department of Medical Biochemistry and Biophysics, Karolinska Institutet, Stockholm, Sweden. ⁶Molecular and Cellular Exercise Physiology, Department of Physiology and Pharmacology, Karolinska Institutet, SE-17177 Stockholm, Sweden. ⁷Steno Diabetes Center Odense, Odense University Hospital, Odense, Denmark. ⁸Department of Biology, University of Copenhagen, Copenhagen, Denmark. ⁹Charles Perkins Centre, School of Life and Environmental Sciences, University of Sydney, Sydney, New South Wales, Australia. ¹⁰Institute of Sports Medicine Copenhagen, Department of Orthopaedic Surgery M, Bispebjerg Hospital, Copenhagen, Denmark. ¹¹Center for Healthy Aging, Faculty of Health and Medical Sciences, University of Copenhagen, Copenhagen, Denmark. ¹²Department of Sports Science and Clinical Biomechanics, University of Southern Denmark, Odense, Denmark. ¹³Clinical Research Centre, Medical University of Bialystok, Bialystok, Poland. ¹⁴Department of Clinical Research, University of Southern Denmark, Odense, Denmark. ¹⁵Institute for Mitochondrial Diseases and Aging, Cologne Excellence Cluster on Cellular Stress Responses in Aging-Associated Diseases (CECAD) and Center for Molecular Medicine (CMMC), Medical Faculty, University of Cologne, Cologne, Germany.

 e-mail: Lykkesylow@sund.ku.dk